TALMA DUARTE FREITAS

TERMODINÂMICA E CINÉTICA DE INTERAÇÃO INTERMOLECULAR ENTRE PROTEÍNAS E COMPOSTOS FÉNOLICOS

Dissertação apresentada à Universidade Federal de Viçosa, como parte das exigências do Programa de Pós-Graduação em Ciência e Tecnologia de Alimentos, para obtenção do título de *Magister Scientiae*.

Orientador: Ana Clarissa dos Santos Pires

Coorientadores: Luís Henrique M. da Silva
Jaqueline de Paula Rezende

VIÇOSA - MINAS GERAIS
2022

Ficha catalográfica elaborada pela Biblioteca Central da Universidade Federal de Viçosa - Campus Viçosa

T
F866t
2022

Freitas, Talma Duarte, 1995-
Termodinâmica e cinética de interação intermolecular entre proteínas e compostos fenólicos / Talma Duarte Freitas. – Viçosa, MG, 2022.
1 dissertação eletrônica (92 f.): il. (algumas color.).

Orientador: Ana Clarissa dos Santos Pires.
Dissertação (mestrado) - Universidade Federal de Viçosa, Departamento de Tecnologia de Alimentos, 2022.
Inclui bibliografia.
DOI: https://doi.org/10.47328/ufvbbt.2022.243
Modo de acesso: World Wide Web.

1. Compostos bioativos. 2. Proteínas. 3. Fenóis. 4. Análise espectral. 5. Fluorescência. 6. Ressonância. I. Pires, Ana Clarissa dos Santos, 1981-. II. Universidade Federal de Viçosa. Departamento de Tecnologia de Alimentos. Programa de Pós-Graduação em Ciência e Tecnologia de Alimentos. III. Título.

CDD 22. ed. 572.696

Bibliotecário(a) responsável: Euzebio Luiz Pinto CRB 6/3317

TALMA DUARTE FREITAS

TERMODINÂMICA E CINÉTICA DE INTERAÇÃO INTERMOLECULAR ENTRE PROTEÍNAS E COMPOSTOS FÉNOLICOS

Dissertação apresentada à Universidade Federal de Viçosa, como parte das exigências do Programa de Pós-Graduação em Ciência e Tecnologia de Alimentos, para obtenção do título de *Magister Scientiae*.

APROVADA: 11 de fevereiro de 2022.

Assentimento:

Talma Duarte Freitas

Autora

Ana Clarissa dos Santos Pires

Orientadora

AGRADECIMENTOS

Agradeço primeiramente a Deus por ser meu guia e me proporcionar muita força em todas as minhas caminhadas ao longo da vida.

Ao meu pai e minha mãe por serem meus exemplos de força e superação. Às minhas irmãs Aline, Ariane e Tainá, por todo apoio, carinho e paciência durantes os anos em que voltei para Viçosa.

À Professora Ana Clarissa (orientadora) por toda ajuda e paciência em me ensinar e orientar da melhor forma. Além disso, por estar sempre pronta para ajudar e compreender as dificuldades e necessidades dos seus orientandos.

Ao Professor Luís Henrique pela participação como coorientador e todos os conhecimentos proporcionados ao longo do mestrado.

À Professora Jaqueline pela participação como coorientadora e por todo auxílio e ensinamentos oferecidos durantes os anos de mestrado. Toda ajuda e companheirismo foram extremamente importantes ao longo do mestrado!

À Professora Márcia e Dra. Eliara por aceitarem participar da banca de defesa e pelas importantes contribuições para este trabalho.

Aos meus amigos e companheiros de trabalho do grupo THERMA, em especial Lívia, Jaqueline e Rafaela, pela convivência, amizade e suporte em todas as atividades do laboratório e do mestrado como um todo.

Ao grupo QUIVECOM, pela parceria nos trabalhos e disponibilização de equipamentos e reagentes.

À Universidade Federal de Viçosa (UFV) e ao Departamento de Tecnologia de Alimentos, pela possibilidade de realizar o Mestrado em Ciência e Tecnologia de Alimentos.

À Coordenação de Aperfeiçoamento de Pessoal de Nível superior – Brasil (CAPES), pela concessão da bolsa de estudo.

O presente trabalho foi realizado com apoio do Conselho Nacional de Desenvolvimento Científico e Tecnológico (CNPq) e Fundação de Amparo à Pesquisa do Estado de Minas Gerais (FAPEMIG).

BIOGRAFIA

TALMA DUARTE FREITAS, filha de José Luís de Paiva Freitas e Lúcia Helena Duarte Freitas, nasceu em Humaitá, Amazonas, em 12 de maio de 1995.

Em outubro de 2013, iniciou o Curso de Engenharia de Alimentos na Universidade Federal de Lavras, graduando-se em julho de 2019.

Em agosto de 2019, iniciou o Mestrado no Programa de Pós-Graduação em Ciência e Tecnologia de Alimentos na Universidade Federal de Viçosa.

Em fevereiro de 2022 defendeu sua dissertação de mestrado.

RESUMO

FREITAS, Talma Duarte, M.Sc., Universidade Federal de Viçosa, fevereiro de 2022. **Termodinâmica e cinética de interação intermolecular entre proteínas e compostos fenólicos.** Orientadora: Ana Clarissa dos Santos Pires. Coorientadores: Luís Henrique Mendes da Silva e Jaqueline de Paula Rezende.

Os compostos fenólicos, como o ácido tânico (AT), Naringina (NR) e Naringenina (NG) são potenciais ingredientes funcionais devido aos seus efeitos nutracêuticos, mas limitações dificultam suas aplicações na indústria. Uma alternativa interessante para minimizar essas dificuldades é complexação destes compostos com proteínas (alfa-amilase (α-am), alfa-lactoalbumina (α-La) e Lisozima (Lys)). Essas moléculas são consideradas excelentes moléculas transportadoras, visto que podem apresentar alto valor nutricional, boas propriedades sensoriais, baixa toxicidade e capacidade de interagirem com compostos hidrofóbicos. A interação de compostos fenólicos com proteínas pode ser afetada por diferentes fatores (flexibilidade estrutural das moléculas, abundância de grupos hidroxila dos compostos fenólicos e quantos sítios de interação a proteína terá para determinado ligante). O estudo da termodinâmica e cinético de formação de complexos permite obter informações sobre a dinâmica do processo de interação e seus interferentes. Portanto, neste trabalho foi apresentado no capítulo 1 o estudo termodinâmico dos complexos α-LA-AT, α-am-AT e Lis-AT, nas temperaturas de 293,15 a 313,15 K, utilizando a espectroscopia de fluorescência. A estequiometria complexa (n) é aproximadamente 1:1 para Lys-AT e 1:2 para α-am-AT e α-La-AT, enquanto a constante de ligação (K_b) é da ordem de 10^5 M^{-1} para todas proteínas. O aumento da temperatura diminui os valores de K_b dos complexos α-am-AT e Lys-AT e aumenta os valores de K_b do complexo α-La-AT. A formação do complexo é conduzida entalpicamente e entropicamente para o α-am–AT e Lys–AT, respectivamente, e conduzida entropicamente para a ligação α-La-AT. Essas informações confirmam o quão importante é o estudo termodinâmica da interação de um composto fenólico com as diferentes proteínas, visto que foi possível perceber que o AT interage por diferentes mecanismos com proteínas distintas. Por fim, no capítulo 2 foi apresentado um artigo científico que expõe o efeito da hidrofobicidade nas

interações da α-LA com NR e NG, através do estudo termodinâmico e cinético, por meio da ressonância plasmônica de superfície e também foram realizadas análises utilizando a técnica de *docking* molecular. Os resultados demonstraram que a constante de taxa de associação entre α-La e NR foi aproximadamente três vezes maior do que entre α-La e NG, e a constante de taxa de dissociação foi menor para α-La–NG do que para α-La–NR em todas as temperaturas avaliadas. A análise termodinâmica revelou que o mecanismo de formação de α-La–NG foi predominantemente entrópico devido ao processo de dessolvatação para acessar sítios hidrofóbicos. Entretanto, a presença do grupo glicosídeo em NR promoveu interações hidrofílicas. O melhor modelo de ligação produzido por *docking* molecular sugeriu que ambas as moléculas se ligam à mesma cavidade proteica.

Palavras-chave: Compostos bioativos. Espectroscopia de Fluorescências. Ressonância Plasmônica de Superfície. Complexos Moleculares.

ABSTRACT

FREITAS, Talma Duarte, M.Sc., Universidade Federal de Viçosa, February, 2022. **Thermodynamics and kinetics of intermolecular interaction between proteins and phenolic compounds**. Advisor: Ana Clarissa dos Santos Pires. Co-advisors: Luís Henrique Mendes da Silva and Jaqueline de Paula Rezende.

Phenolic compounds such as tannic acid (AT), Naringin (NG) and Naringin (NG) are functional ingredients because they have nutraceutical effects. However, there are some difficulties in the application of these compounds in the industry. An interesting alternative to minimize these difficulties is the formation of complexes of these compounds with proteins (alpha-amylase (α-am), alpha-lactoalbumin (α-La) and Lysozyme (Lys)). Proteins are considered excellent carrier molecules, may have high nutritional value, good sensory properties, low toxicity and ability to interact with hydrophobic compounds. The interaction of phenolic compounds with proteins can be affected by different factors (structural flexibility of the molecules, abundance of hydroxyl groups of phenolic compounds and how many interaction sites the protein will have for a given ligand). The study of thermodynamics and kinetics of complex formation allows obtaining information about the dynamics of the interaction process and its interferents. Therefore, in Chapter 1, the thermodynamic study of the α-LA-AT, α-am-AT and Lys-AT complexes, at temperatures from 293.15 to 313.15 K, using fluorescence spectroscopy was presented. The stoichiometry (n) is approximately 1:1 for Lys-AT and 1:2 for α-am-AT and α-La-AT, while the binding constant (K_b) is on the order of 10^5 M^{-1} for all proteins. Increasing the temperature decreases the K_b values of the α-am-AT and Lys-AT complexes and increases the K_b values of the α-La-AT complex. Complex formation is conducted enthalpically and entropy for α-am–AT and Lys–AT and conducted entropically for α-La-AT. This information confirms how important the thermodynamic study of the interaction of a phenolic compound with different proteins is, because it was possible to perceive that AT interacts by different mechanisms with different proteins. Finally, in chapter 2, a scientific article was presented that exposes the effect of hydrophobicity on the interactions of α-LA with NR and NG, through the thermodynamic and kinetic study, using the surface plasmon resonance technique and analyzes were also performed using the technique of molecular docking. The results showed that the association rate constant between α-

La and NR was approximately three times higher than between α-La and NG, and the dissociation rate constant was lower for α-La–NG than for α- La–NR at all temperatures evaluateds. Thermodynamic analysis revealed that the mechanism of α-La–NG formation was predominantly entropic due to the desolvation process to access hydrophobic sites. In contrast, the presence of the glycoside group in NR promoted hydrophilic interactions. The best binding model produced by molecular docking suggested that both molecules bind to the same protein cavity.

Keywords: Bioactive compounds. Fluorescence Spectroscopy. Surface Plasmonic Resonance. Molecular Complexes.

SUMÁRIO

INTRODUÇÃO GERAL

Os compostos fenólicos pertencem à uma das classes de moléculas bioativas mais utilizados em produtos nutracêuticos, devido as suas inúmeras propriedades promotoras da saúde (antioxidante, antibacteriana, antiviral, anti-inflamatória, dentre outras). Esses compostos são as principais substâncias formadas pelo metabolismo secundário das plantas e são divididos em diferentes grupos: ácidos fenólicos, flavonóides, taninos, estilbenos e lignanas (BOUDET, 2007).

A naringina (NR) e naringenina (NG) são dois dos mais importantes flavonóides de ocorrência natural, encontrados em algumas frutas comestíveis, como espécies cítricas (laranja, limão, toranja), tomates e figos. Quimicamente a NR é conhecida como 4',5,7-trihydroxyflavanone 7-rhamnoglucoside e sua aglicona, NG, como 2,3-di-hidro-5,7-dihidroxi-2-(4-hidroxifenil)-4H-1-benzopiran-4-ona. As massas molares da NR e NG são 580,54 e 272,26 g/mol, respectivamente. Ambas moléculas são pouco solúveis em água, mas são muito solúveis em solventes orgânicos como álcool. Além disso, são dotadas de amplos efeitos biológicos na saúde humana, que inclui atividade antioxidante, antimicrobiano, anti-inflamatório, antiviral (hepatite C, Chikungunya e dengue), anti-alzheimer, anti-câncer, anti-asma e outros (SALEHI et al., 2019).

O ácido tânico (AT) é um composto pertencente ao grupo dos taninos, que possui massa molar igual 1.701,19 g/mol. Esta molécula é miscível em água, muito solúvel em álcool e acetona e insolúvel em éter, benzeno, tetracloreto de carbono e clorofórmio. As principais fontes comestíveis de AT são as uvas, romã, açaí, vinho e chá preto. Além disso, possui propriedades antioxidantes, antimutagênicas, antitumorais e apresenta atividade contra microrganismos (bactérias e vírus) (BAER-DUBOWSKA et al., 2020; KACZMAREK, 2020).

Apesar dos potenciais aplicações destas moléculas bioativas em diferentes matrizes, as indústrias enfrentam desafios ao utilizar esses compostos, visto que alguns apresentam baixa solubilidade em meio aquoso, além de serem sensíveis a luz, oxigênio e altas temperaturas. Uma solução pertinente para essa dificuldade é utilização de moléculas carreadoras, como por exemplo as proteínas. A complexação com estas biomoléculas pode viabilizar a veiculação dos compostos bioativos em diferentes matrizes, como alimentos, embalagens bioativas, fármacos e cosméticos.

Diversas proteínas podem ser utilizadas como carreadoras para compostos fenólicos, como a alfa-lactoalbumina (α-La). A α-La é uma proteína globular

encontrada no leite bovino e humano. Esta proteína possui massa molecular correspondente a 14,07 kDa no leite humano e 14,18 kDa no leite bovino e seu conteúdo no soro bovino é de aproximadamente 1,2 g/L. Além disso, apresenta cadeia simples composta por 123 aminoácidos, dentre estes destacam-se a presença de aminoácidos essenciais como triptofano (Trp), lisina (Lis) e cisteína (Cis). Os principais destaques da α-La é sua baixa toxicidade e a capacidade de interagir com substâncias hidrofóbicas, permitindo que esta seja transportadora de compostos fenólicos como NR e NG (PERMYAKOV; BERLINER, 2000).

A lisozima (Lys) é uma proteína globular monomérica que possui massa molecular igual a 18,7KDa. Apresenta em sua estrutura cerca de 129 resíduos de aminoácidos, dentre os quais, seis são resíduos de Trp. Geralmente é encontrada em vários fluidos secretores, como leite humano, lágrimas, muco, saliva, e etc. Também, pode ser encontrada em outras fontes, como em claras de ovo de galinha. A Lys apresenta diferentes funções farmacêuticas e fisiológicas, por exemplo, antitumoral, antiviral, anti-histamínica, anti-inflamatória, antimicrobiana e antisséptica. Além de suas funções farmacêuticas, apresenta um papel importante como proteína transportadora, e pode se ligar a uma variedade de compostos bioativos como beta-caroteno, luteína, NR, NG e AT (DAS et al., 2018a; MAGALHÃES et al., 2021b; REZENDE et al., 2020c; SU et al., 2019).

A alfa-amilase (α-am) é um dos principais constituintes da saliva, representando de 10 a 20% de todas as proteínas encontradas. É formada por duas famílias de isoenzimas, onde uma é glicosilada e a outra não apresenta carboidratos em sua estrutura. A massa molar da forma glicosilada é de em torno de 57 kDa, já a da forma não glicosilada é de aproximadamente 54 kDa. Ademais, é composta por 512 aminoácidos e possui intensidade de fluorescência consequente de seus aminoácidos fluoróforos intrínsecos, Trp, Tirosina (Tyr) e fenilalanina (Phe). Na literatura já foi relatado que α-am é capaz de interagir com o AT que, consequentemente, inibe sua atividade frente a digestão da glicose. Ou seja, a interação destas duas moléculas no organismo podem proporcionar efeitos antidiabéticos (KANDRA et al., 2004).

A interação de compostos fenólicos com proteínas pode ser afetada por diferentes fatores, como por exemplo: a flexibilidade estrutural das moléculas, abundância de grupos hidroxila dos compostos fenólicos e quantos sítios de interação a proteína possui para determinado ligante. Fatores externos como as condições de

processamentos (temperatura, pH e etc) e a digestibilidade no trato gastrointestinal ((BUITIMEA-CANTÚA; GUTIÉRREZ-URIBE; SERNA-SALDÍVAR, 2018) também podem influenciar na interação. O estudo da termodinâmica e cinética de formação de complexos permite obter informações valiosas sobre a dinâmica do processo de interação e seus interferentes, e assim, otimizar e aperfeiçoar suas aplicações na indústria.

A espectroscopia de fluorescência (FS) é uma técnica comumente utilizada para determinar os parâmetros termodinâmicos de formação de complexo (variação da energia livre de Gibbs padrão (ΔG°), a variação da entalpia padrão (ΔH°) e a variação da entropia padrão (ΔS°)). A FS é eficiente para avaliar a interação de compostos fenólicos com proteínas, porque muitas proteínas possuem resíduos de aminoácidos fluoróforos, como Trp, Tyr e a Phe. Além disso, é possível obter informações sobre alterações conformacionais da proteína, bem como sobre a vizinhança dos seus fluoróforos.

Através da técnica de FS, UV-visível e calorimetria de titulação isotérmica (ITC), Ishtikhar et al., (2018) estudaram a termodinâmica da interação de AT com albuminas séricas homólogas de mamíferos (HSAM). De acordo com resultados obtidos por FS ($\Delta G^{\circ}_{288\,K} = -37{,}95\ kcal\ mol^{-1}$, $\Delta H^{\circ}_{288\,K} = -37{,}80\ kcal\ mol^{-1}$, e $T\Delta S^{\circ}_{288\,K} = 147{,}0\ \mathrm{cal}\ mol^{-1}$), AT interage especificamente em mais de um sítio de ligação das HSAM, sendo as interações hidrofóbicas as principais responsáveis pela formação do complexo.

Yazdani et al., (2022), também utilizaram a FS para estudar a interação da NG e albumina sérica bovina (BSA). Os autores concluíram que ao interagir com a NG, a proteína pode desdobrar sua estrutura e aumentar a exposição dos grupos cromóforos na área hidrofóbica interior. Além disso, os resultados termodinâmicos ($\Delta G^{\circ}_{293\,K} = -25{,}65\ kJ\ mol^{-1}$, $\Delta H^{\circ}_{293\,K} = -55{,}54\ kJ\ mol^{-1}$, e $\Delta S^{\circ}_{293\,K} = -101{,}00\ J\ mol^{-1}$) revelaram que as ligações de hidrogênio são a principais forças que governam a interação dessas moléculas.

Outra técnica interessante para realizar estudos termodinâmicos de formação de complexos envolvendo proteínas é a Ressonância Plasmônica de Superfície (RPS). Por meio desta técnica é possível investigar a interação de um ligante com proteínas que não apresentam aminoácidos fluorófulos em sua estrutura. Além disso, utiliza pequena quantidade de reagentes e permite realizar o estudo cinético da formação dos complexos. Pacheco et al. 2020, estudaram a interação da Beta-

caseína (β-cas) com a NR, avaliando o seu uso como proteína carreadora, utilizando as técnicas FS e RPS. Os resultados obtidos por RPS ($\Delta G^{\circ}_{293\,K} = -21{,}50\ kJ\ mol^{-1}$, $\Delta H^{\circ}_{293\,K} = 6{,}85\ kJ\ mol^{-1}$, e $T\Delta S^{\circ}_{293\,K} = 28{,}35\ kJ\ mol^{-1}$) demonstraram que a β-cas forma complexos com a NR e o processo de ligação β-cas–NR ocorre principalmente devido as interações hidrofóbicas.

Os compostos fenólicos são potenciais ingredientes funcionais devido aos seus efeitos nutracêuticos, mas a instabilidade à luz, diferentes pH, elevadas temperaturas e baixa solubilidade em meio aquoso limitam suas aplicações na indústria. A complexação destas moléculas com as proteínas é uma alternativa interessante para minimizar essas dificuldades, visto que as proteínas são consideradas excelentes moléculas transportadoras, possuem alto valor nutricional, boas propriedades sensoriais, baixa toxicidade e capacidade de interagirem com compostos hidrofóbicos. Na literatura já foram realizadas diversas investigações das interações de compostos fenólicos e diferentes proteínas. Porém, ainda existem sistemas importantes que não foram analisados e necessitam de estudos termodinâmicos e cinéticos, como por exemplo α-LA-NR, α-LA-NG, α-LA-AT, α-am-AT e Lis-AT.

Neste sentido, a presente dissertação tem como objetivo uma ampla abordagem sobre a interação dos sistemas α-LA-NR, α-LA-NG, α-LA-AT, α-am-AT e Lis-AT. Para isso, o trabalho foi dividido em duas partes: a primeira é um capítulo que a aborda o estudo termodinâmico dos complexos α-LA-AT, α-am-AT e Lis-AT, nas temperaturas de 293,15 a 313,15 K, utilizando a FS. Enquanto a segunda, é um artigo científico que expõe o efeito da hidrofobicidade da NR e NG nas interações com α-LA, através do estudo termodinâmico e cinético, por meio da RPS.

.

CAPÍTULO 1 – Complexos de ácido tânico-proteínas: Uma abordagem termodinâmica

RESUMO

O ácido tânico (AT) é uma molécula bioativa com propriedades funcionais, como atividade antidiabética, antimutagênica e antimicrobiana. No entanto, apresenta algumas limitações, como sabor amargo e sensação adstringente no paladar, que reduzem sua aceitação pelos consumidores. O AT pode formar complexos com proteínas, e essa capacidade pode ser útil para entregar essa importante molécula a diferentes matrizes. Aqui, apresentamos uma abordagem termodinâmica para a formação de um complexo entre AT e proteínas (alfa-amilase (α-am), alfa-lactoalbumina (α-La) e lisozima (Lys)) relevantes nas áreas alimentícia e farmacêutica. A espectroscopia de fluorescência é usada para obter os parâmetros termodinâmicos para a formação do complexo. A estequiometria complexa (n) é aproximadamente 1:1 para Lys-AT e 1:2 para α-am-AT e α-La-AT, enquanto a constante de ligação (K_b) é da ordem de 10^5 M^{-1} para todos proteínas. O aumento da temperatura diminui os valores de K_b dos complexos α-am-AT e Lys-AT e aumenta os valores de K_b do complexo α-La-AT. A formação do complexo é conduzida entalpicamente e entropicamente ($\Delta H^0 < 0$ and $T\Delta S^0 > 0$) para o α-am–AT e Lys–AT, respectivamente, e conduzida entropicamente ($\Delta H^0 > 0$ and $T\Delta S^0 > 0$) para a ligação α-La-AT. O conhecimento dos parâmetros termodinâmicos pode fornecer informações relevantes para entender as forças motrizes para formar complexos com AT e selecionar a melhor proteína para carrear AT. Além disso, este estudo pode contribuir para o desenvolvimento de nutracêuticos para melhorar a digestão do amido.

CHAPTER 1 – Tannic Acid-Protein complexes: A thermodynamic approach

ABSTRACT

Tannic acid (TA) is a bioactive molecule with functional properties, such as antidiabetic, antimutagenic, and antimicrobial activities. However, it exhibits some limitations, such as bitter taste and astringent sensation on the palate, which reduce its acceptance by consumers. TA can form complexes with proteins, and this ability may be useful for delivering this important molecule to different matrices. Herein, we present a thermodynamic approach to the formation of a complex between TA and proteins (alpha-amylase (α-am), alpha-lactoalbumin (α-La), and lysozyme (Lys)) relevant in the food and pharmaceutical fields. Fluorescence spectroscopy is used to obtain the thermodynamic parameters for the complex formation. The complex stoichiometry (n) is approximately 1:1 for Lys–TA and 1:2 for α-am–TA and α-La–TA, while the binding constant (K_b) is in the order of 10^5 M^{-1} for all proteins. Increasing the temperature decreases the K_b values of the α-am–TA and Lys–TA complexes and increases the K_b values of the α-La–TA complex. The formation of the complex is enthalpically and entropically driven ($\Delta H^0 < 0$ and $T\Delta S^0 > 0$) for the α-am–TA and Lys–TA, respectively, and entropically driven ($\Delta H^0 > 0$ and $T\Delta S^0 > 0$) for the α-La–TA binding. Knowledge of the thermodynamic parameters can provide relevant information to understand the driving forces to form complexes with TA and select the best protein to carry TA. Additionally, this study can contribute to the development of nutraceuticals for improved starch digestion.

.

1. Introduction

The current pandemic has caused the population to seek new habits. There is increased attention to hygiene, social isolation, and better quality of life (including physical exercise and healthy eating) (Esobi et al., 2020). Although there are no foods capable of fully immunizing against viruses and bacteria, healthy foods rich in bioactive compounds contribute to the fortification of the immune system to fight the symptoms of viral contamination in the body (ABBAS et al., 2021; Seres & Coates, 2021). Faced with the current demand, industries are looking to include functional ingredients, such as phenolic compounds (PC), in their products.

The PC is one of the most abundant classes of bioactive molecules. Tannins are one of the main groups of PCs and can be divided into two subclasses: hydrolyzable tannins and condensed tannins. Tannic acid (TA) is one of the simplest hydrolyzable tannins. It has important bioactivities, such as antioxidant and antitumor properties, and is active against microorganisms (bacteria and viruses) (Kaczmarek, 2020).

Although TA has several functional properties, it shows bitter taste and astringent sensation on the palate, which can impair the consumption of a particular food product when this bioactive compound is added (Soares et al., 2020). Astringency, like bitterness, is perceived as a negative attribute and cited as the reason consumers reject nutraceuticals despite their known health benefits (Lesschaeve & Noble, 2005). It has been reported that the interaction between lactoferrin (bovine milk protein) and naringenin (PC found in grapefruit and citrus fruits) reduces the maximum bitterness intensity and the overall perception of bitterness for naringenin by 27% and 33%, respectively (Nunes et al., 2020). Thus, a possible alternative to mask the bitterness and improve the sensory appeal of PC is its complexation with macromolecules, such as proteins.

Proteins and PC can interact through different mechanisms and suffer interference because of the chemical structure and flexibility of biomolecules and different thermodynamic conditions, such as temperature and pH. To understand the nature of the complex formation between proteins and different ligands, it is necessary to understand the system at the molecular level. Through the study of thermodynamic parameters (binding constant (K_b), complex stoichiometry (n), standard Gibbs free energy change ($\Delta G°$), standard enthalpy change ($\Delta H°$), and standard entropy change

(TΔS°)), it is possible to obtain information on the main mechanisms responsible for the complexation of these molecules and how the environmental conditions interfere with this interaction (Chen et al., 2021).

Fluorescence spectroscopy (FS) is a technique widely used for interaction studies, mainly between phenolic compounds and proteins that contain fluorophore amino acids in their structure. This technique allows us to obtain information on the thermodynamic parameters of the interaction between the analyte and the region of the protein in which the fluorophore is located. When the interaction between these molecules occurs, the fluorescence intensity of the protein may be suppressed in a process called fluorescence quenching (Santa Rosa et al., 2021).

Some studies have evaluated the interactions between TA and different proteins using FS. Xiao et al. (2015) have investigated the interactions of TA with α-glucosidase (α-gly) and trypsin (Tryp) enzymes. The authors have found that there is a decrease in α-gly and Tryp activity in the presence of TA. Additionally, the results indicate that the main driving forces to form TA complexes with α-gly ($\Delta G^{\circ}_{298\,K} = -31.55\ kJ/mol$, $\Delta H^{\circ}_{298\,K} = 3.32\ kJ/mol,$ and $\Delta S^{\circ}_{298\,K} = 213.10\ kJ/molK$) and Tryp ($\Delta G^{\circ}_{298\,K} = -37.02\ kJ/mol$, $\Delta H^{\circ}_{298\,K} = 8.33 kJ/mol$, and $\Delta S^{\circ}_{298\,K} = 147.30\ kJ/mol\,K$) are the hydrophobic and electrostatic interactions. Jing et al. (2021) have studied the thermodynamics of the interaction between TA and bovine lactoferrin (LF). The results obtained ($\Delta G^{\circ}_{298\,K} = -30.34\ kJ/mol$, $\Delta H^{\circ}_{298\,K} = 7.93\ kJ/mol$, and $\Delta S^{\circ}_{298\,K} = 128.5\ kJ/molK$) reveal that TA can bind to LF mainly through hydrophobic interaction. Although there have been studies on the interaction between TA and some proteins, a thermodynamic study of the interaction with alpha-amylase (α-am), alpha-lactoalbumin (α-La), and lysozyme (Lys) has not yet been reported. These proteins are relevant because of their functions, such as the transport of hydrophobic molecules (Magalhães et al., 2021; Permyakov & Berliner, 2000; Rezende et al., 2020), antimicrobial activity (Hamdani et al., 2018; Vilcacundo et al., 2018), and starch digestion (Avwioroko et al., 2020; Hui et al., 2020; Sun et al., 2016).

The α-am is part of a class of hydrolases that act directly on the glycosidic bonds of starch. Therefore, they play a key role in food digestion. It has been reported in the literature that TA can interact with α-am, inhibiting the activity of this enzyme against glucose digestion, demonstrating its potential anti-diabetic effect. However, the mechanism of the interaction between these two molecules, which can contribute to

enhancing the use of TA by the pharmaceutical industry, is still unknown (Lou et al., 2018; Tiemi et al., 2019).

The α-La is a globular protein found in bovine and human milk. Bovine α-La accounts for approximately 20% to 25% of whey proteins (Kamau et al., 2010). This protein exhibits good emulsifying and foaming properties. Additionally, it has antihypertensive, antimicrobial, anticancer, prebiotic, and immunomodulatory effects; therefore, it is considered a bioactive peptide (Mohammadi & Moeeni, 2015a). A homologous protein of a-La is Lys, which is also found in human milk (0.2–0.4 mg/mL) and bovine milk (0.05–0.22 µg/mL); however, one of the main sources is chicken egg (60–120 mg/mL) (Forsythe et al., 1999; Yang et al., 2011). Lys can bind to bioactive compounds, such as beta-carotene and lutein (Magalhães et al., 2021; Rezende et al., 2020). Further, it has various health-promoting activities, including antitumor, antiviral, antihistamine, anti-inflammatory, antimicrobial, and antiseptic properties (Kamau et al., 2010).

The technological and functional functions of α-am, α-La, and Lys are important in the food and pharmaceutical sectors; thus, the objective of this book is to present a thermodynamic approach to the interaction of TA with these proteins.

Therefore, using the FS technique, a thermodynamic study (calculating the K_b, n, $\Delta G°$, $\Delta H°$, and $T\Delta S°$) of the formation of α-am–TA, α-La–TA, and Lys–TA at temperatures of 293.15, 298.15, 303.15, 308.15, and 313.15 K is carried out.

2. Tannic Acid

Polyphenols constitute a large group of organic compounds with a wide range of complex structures. They contain numerous phenolic rings with predominant carboxylic and hydroxyl groups. They are divided into phenolic acids, flavonoids, tannins, stilbenes, and lignans. Additionally, they are naturally biosynthesized by various plants and fruits from which they are commonly extracted (Kim et al., 2010).

TA (Figure 1) is a tannin with a molar mass of 1,701.19 g/mol, and its structure consists of a central glucose unit and ten gallic acid molecules. The main edible sources of TA are grapes, pomegranates, açaí, wine, and black tea. This molecule is miscible with water, highly soluble in alcohol and acetone, and insoluble in ether, benzene, carbon tetrachloride, and chloroform (Kaczmarek, 2020).

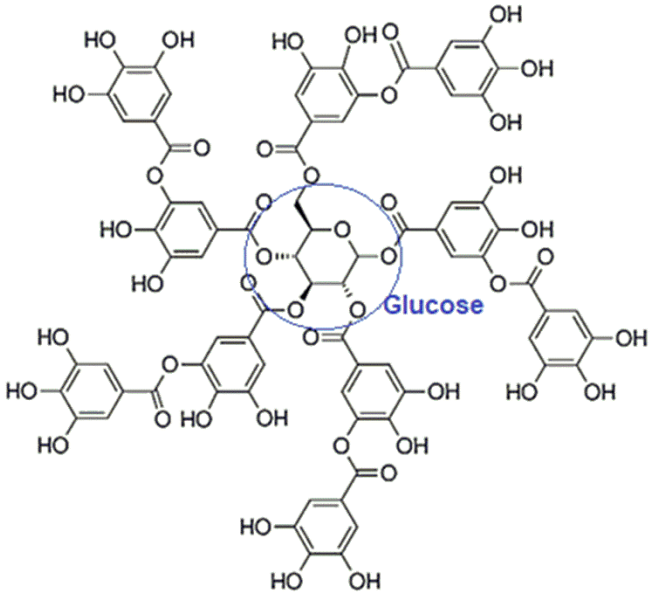

Figure 1. Chemical structure of TA.

TA has several nutraceutical properties, such as antimutagenic, antidiabetic, and homeostatic properties. This compound can neutralize free radicals that cause the development of different diseases, such as allergies, Parkinson's disease, Alzheimer's disease, and cardiovascular diseases (Belhaoues et al., 2020; Kaczmarek, 2020). In addition to its bioactive functions, this molecule plays an important role in antimicrobial activity against pathogenic bacteria, such as Salmonella typhimurium and Escherichia coli (Kaczmarek, 2020; Kim et al., 2010).

The bioactivity of TA has attracted interest in the pharmaceutical and food industries. However, its application presents major technological challenges (such as bitter taste) that can be overcome using approaches such as complexation with other molecules. Thus, food proteins are being increasingly investigated for their potential use as delivery vehicles for bioactive compounds because of their biocompatibility, cost-effectiveness, and availability (De Wit, 1998).

3. Proteins

3.1 α-am

Amylases are a class of hydrolases that act directly on the glycosidic bonds of starches. Among the amylases, α-am (Figure 2) is the most abundant protein found in

saliva, representing 10% to 20%. Additionally, they may originate from fungi and bacteria. The protein denaturation temperature is approximately 348.15 to 368.15 K (Violet & Meunier, 1989). The molar mass varies from 10 to 210 kDa, depending on its origin: 54 to 62 kDa from saliva, 41 to 69 kDa from fungi, and 28 to 78 kDa from bacteria (Ji et al., 2021). The isoelectric points of the different α-am have similar values: 6.6 and 6.9 for bacterial and salivary protein, respectively (Company, 1975; Faber et al., 2007).

Figure 2. Structure of human salivary α-am.

The α-am is composed of 512 amino acids and has a fluorescence intensity resulting from its intrinsic fluorophore amino acids, tryptophan (Trp), tyrosine (Tyr), and phenylalanine (Phe). The α-am from the porcine pancreas has approximately 19 Trp residues, which is the highest number compared to the α-am from Aspergillus oryzae (10 residues) and Bacillus licheniformis (17 residues) (Duy & Fitter, 2006).

The inhibitors of α-am slow the digestion of carbohydrates, and this reduces the rate of glucose absorption, which in turn lowers postprandial blood glucose levels. Therefore, delaying starch digestion by inhibiting enzymes, such as α-am, may play an important role in diabetes control (Bhargava et al., 2021; Tingting Wu et al., 2011).

Currently, inhibitors already exist; however, they cause several side effects (flatulence, diarrhea, and abdominal pain) as they inhibit α-am excessively. Therefore, an increasing number of studies are being carried out (mainly with phenolic

compounds) to identify safe inhibitors with minimal side effects. Among these polyphenols, TA stands out for its ability to inhibit α-am activity (Abdelli et al., 2021; Lou et al., 2018).

Although the inhibitory effect of TA on α-am has been recognized, little is known about the driving forces for their interaction. Understanding the thermodynamic parameters related to the formation of the α-am–TA complex under different thermodynamic conditions can be strategic for optimizing the inhibitory effect of the TA.

3.2 Lys

The Lys is a monomeric protein with a molecular mass of 14.3 kDa, isoelectric point of 10.7, and denaturing temperature of 348.15 K. This enzyme was accidentally discovered when Alexander Fleming discovered that a drop of his nasal mucus could cause the lysis of bacteria present in the plate of his experiment, drawing attention to a new bacteriolytic element (Fleming, 1920). Lys has been found in large amounts in human organs, tissues, and secretions (placenta, spleen, tears, saliva, and others). Furthermore, similar lytic enzymes have been isolated from the organs and secretions of various vertebrates, invertebrates, bacteria, and even plants (papaya latex) (Leśnierowski & Yang, 2021).

According to different characteristics, such as structure, catalysis, and immunization, Lys is divided into three dominant families: chicken type (type c), goose type (type g), and invertebrate type (type i). Additionally, several other types of Lys, including phage-type, bacterial-type, and plant-type, have been identified (Wu et al., 2019). The primary structure of the c-type Lys (Figure 3) consists of 129 amino acid residues, which contain four intact disulfide bonds and six Trp, three Tyr, and three Phe residues (Cao et al., 2015).

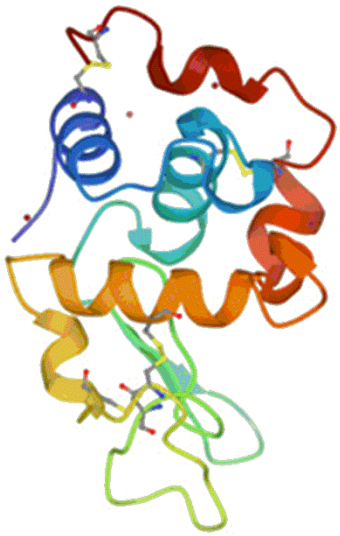

Figure 3. Structure of type c Lys.

The Lys can be used to prevent many bacterial, viral, fungal, and inflammatory diseases (Khan et al., 2022; Tagashira et al., 2018). Additionally, they can inhibit the action of various bacteria, including saprophytic bacteria (Tiantian Wu et al., 2019). Some dangerous bacteria against which Lys has a strong effect are Listeria monocytogenes and Clostridium tyrobutyricum (Vilcacundo et al., 2018). In addition to its pharmaceutical functions, it plays an important role as a carrier protein and can bind to phenolic compounds, such as naringin, naringenin, and TA (Das et al., 2018; Su et al., 2019).

The interaction of Lys with TA affords a powerful antimicrobial complex, as it can inhibit different pathogenic microorganisms. Su et al. (2019) studied the thermodynamics of the Lys and TA interaction. However, they used only two temperatures and applied the Van 't Hoff equation. If the enthalpy and entropy of the complex formation are temperature-dependent, the Van ‘t Hoff graph will not be linear and requires more than three points to observe this. Therefore, it would be interesting to carry out a new thermodynamic study at more than two temperatures.

3.3 α-La

Bovine α-La is quantitatively the second most important whey protein (approximately 1.2 g/L), constituting approximately 20% to 25% of whey proteins. Furthermore, it has a molecular mass corresponding to 14.07 kDa, its isoelectric point

is from 4.2 to 4.6, and the protein is denatured at temperatures above 343.15 K (Nguyen et al., 2017). The structure (Figure 4) of bovine α-La comprises 123 amino acids, including essential amino acids, such as Trp, lysine (Lysi), and cysteine (Cys) (Delavari et al., 2015).

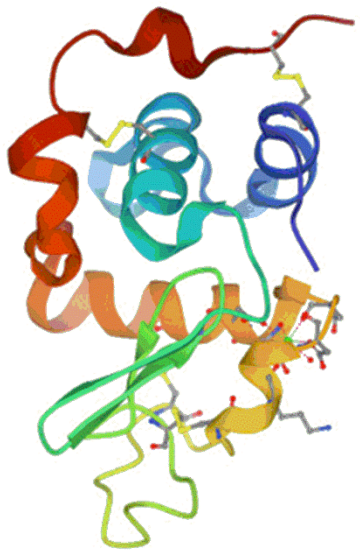

Figure 4. Structure of bovine α-La.

Although α-La is found only in mammalian milk and has a biological function distinct from that of the type c Lys, the two enzymes are closely related. These enzymes show similarities in their amino acid sequences, gene structures, and dimensional conformations, resulting in the placement of α-LA in the same family as type c Lys. Furthermore, accumulating evidence suggests that their encoded genes have evolved from a common progenitor (Brew, 2011).

The α-La has the highest Trp content among all edible protein sources, approximately 6%. This feature allows this molecule to have health- and wellbeing-promoting properties. Trp is an amino acid capable of synthesizing serotonin, a hormone that regulates several fundamental behavioral and physiological functions, including sleep, circadian rhythms, cognition, and mood (Ong et al., 2017).

The α-La can be a delivery vehicle for bioactive compounds because of its low toxicity and ability to interact with hydrophobic substances (Romano et al., 2021). Some studies have shown that α-La effectively binds and transports nutraceuticals, such as vitamin D, genistein, kaempferol, curcumin, epigallocatechin gallate (EGCG), and trans-resveratrol (Delavari et al., 2015; Mohammadi & Moeeni, 2015a, 2015b;

Perusko et al., 2017). Therefore, α-La may be a potential carrier for other bioactive compounds, such as TA. Furthermore, through a thermodynamic study, it is possible to obtain information to optimize the application of this complex in the industry.

4. Fundamentals of fluorescence spectroscopy for the study of intermolecular interactions

Steady-state FS is a useful technique for assaying the intermolecular interactions between small molecules and proteins (He, Chen, Moser, Jones, & Ferruzzi, 2016). This technique offers numerous advantages for the study of molecular interactions and chemical reactions because it is significantly more sensitive than other spectroscopic methods, as fluorescent compounds are highly sensitive to their environment (Shaikh & O'Donnell, 2017).

The fluorescence phenomenon can be understood as the spontaneous emission of photons upon the return of an excited electron to the ground state (Lakowicz, 2006). This phenomenon of fluorescence emission is illustrated in Figure 5, based on the Jablonski diagram.

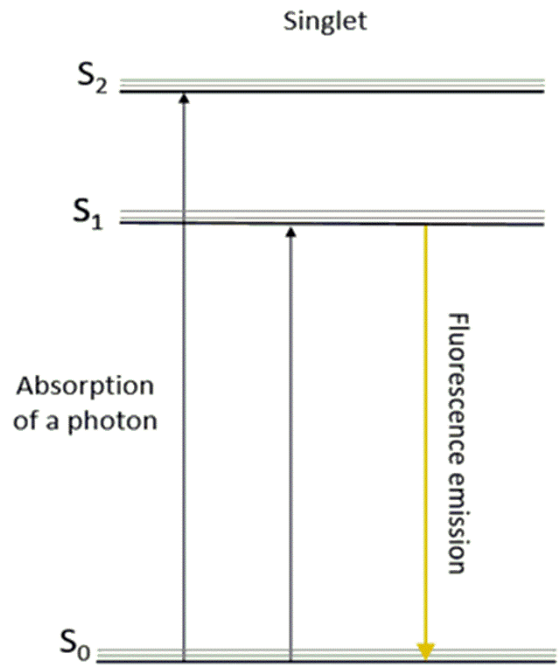

Figure 5. Schematic representation of the fluorescence emission from a fluorophore, based on a simplified Jablonski diagram.

When a fluorophore in its singlet electronic ground (S0) state is excited through energy absorption at a specific wavelength, it can reach the highest vibrational levels of the first or second singlet electronic states (S1 and S2, respectively). A return to the S0 state from the S1 state results in photon emission termed fluorescence, in a process with a lifetime of approximately 10^{-8} s (Lakowicz, 2006).

The fluorophores in the proteins are the amino acids Tyr, Phe, and Trp. The Trp residue is responsible for most of the fluorescence emission of proteins since this amino acid possesses a relatively high molar absorption coefficient and relatively high quantum yield. Further, the fluorescence from Tyr and Phe is useful for investigating protein modifications; however, it has been used far less than that of Trp. This is because they have relatively weak absorptivity, absorb at relatively short wavelengths, have less wavelength sensitivity to the environment, and transfer much of their excitation to Trp if present in the same protein (Callis, 2014a; Nan, Hao, Ye, Feng, & Sun, 2019). Measuring the change in fluorescence emission intensity provides information about conformational and structural changes and the microenvironment of the fluorophores in the protein (Callis, 2014b).

Fluorescence quenching is defined as a decrease in the quantum yield of fluorescence from a fluorophore because of molecular processes, such as energy transfer, molecular rearrangements, collisions, and ground-state complex formation (He et al., 2016). If a quencher molecule interacts with a protein at the site of a fluorophore, i.e., Trp, or in the vicinity of this site, this fluorophore is not excited, and therefore, it does not fluoresce. Thus, the fluorescence intensity signal of the sample is reduced (quenched), as shown in Figure 6.

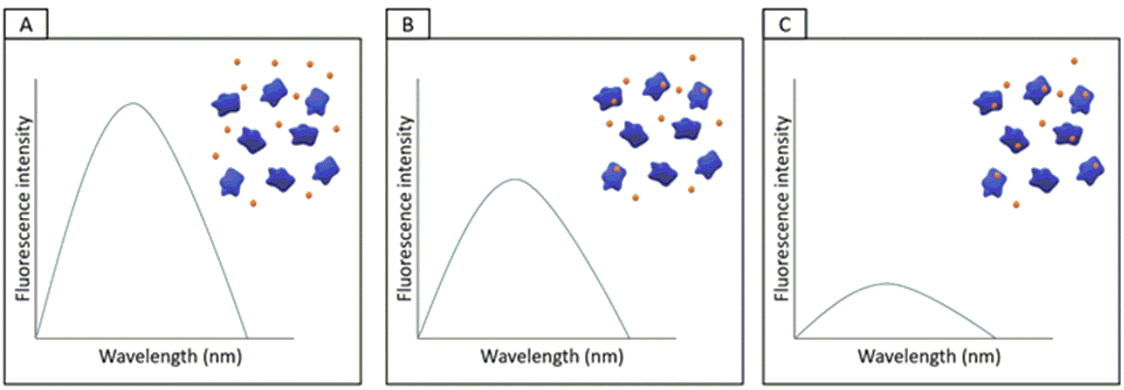

Figure 6. Schematic representation of the fluorescence quenching of fluorophores.

In A, a population of fluorophores (in blue), without interacting with the suppressor molecules (in orange), is represented. In B, part of this population of fluorophores interacts with the quenchers, which results in a reduction in the fluorescence intensity. In C, a further reduction in fluorescence is achieved because of new interactions between the fluorophores and quencher molecules.

The behavior of the fluorescence intensity without and with a quencher can be assessed through a plot of the fluorescence intensity at the emission wavelength (fluorescence spectra), as shown in Figure 6. These fluorescence quenching data, as well as other aspects of the behavior of the obtained spectra, can be used to obtain important information, such as the fluorescence quenching mechanism, the n of the formed complexes, K_b, and the nature of the interactions involved in the formation of the complexes (Bujalowski & Jezewska, 2014).

The fluorescence quenching can be classified as dynamic or static quenching. The dynamic fluorescence quenching mechanism is the result of collisions between a suppressor molecule (quencher) and a fluorophore, which causes the loss of excitation energy. The static quenching mechanism refers to the process of ground-state complex formation between the quencher and fluorophore (Ghosh, Rathi, and Arora 2016). Both static and dynamic quenching mechanisms can coexist during the fluorescence quenching process.

Using the classical Stern–Volmer equation (Eq. 1), the fluorescence quenching mechanism can be distinguished (Lakowicz 2006).

$$\frac{F_0}{F} = \frac{\gamma + k_q[Q]}{\gamma} = 1 + k_q\tau_0[Q] = 1 + K_{sv}\,[Q], \quad (1)$$

where $F\,0$ and F represent the steady-state fluorescence intensities of the fluorophore without and with a quencher, respectively; τ_0 denotes the fluorescence lifetime of the fluorophore (for protein, τ_0 is ordered as 1.0×10^{-8} s); and K_{sv} is the Stern–Volmer constant ($K_{sv} = k_q\tau_0$).

The quenching mechanism can be determined by comparing the biomolecular quenching constant (k_q) with the dynamic quenching rate constant of the maximum scattering collision of several quenchers with biopolymers (2×10^{10} L/mol/s). In general, the quenching mechanism is considered static when the calculated $k_q$value is significantly higher than the rate constant of the collision processes. Moreover, the

K_{sv} values can be used. The K_{sv} of dynamic quenching generally increases with increasing temperature because, in this condition, the diffusion coefficient is relatively high; conversely, if the K_{sv} values decrease with increasing temperature, the quenching mechanism is considered static (Nan et al. 2019). If the static quenching mechanism is predominant in the interaction process between a fluorophore and quencher, the binding and thermodynamic parameters involved in this process can be determined.

A model example for determining the K_b and n of the complex formation between the fluorophore and quencher is presented in Eq. 2.

$$\log\frac{F_0-F}{F} = n\log K_b - n\log\frac{1}{([Q]-\left(\frac{F_0-F}{F_0}\right)[P])}, \quad (2)$$

where F_0 and F are the fluorescence intensities of the fluorophore before and after the addition of the quencher molecule, respectively, [Q] is the total concentration of the quencher, and [P] is the total concentration of the fluorophore. The value of n corresponds to the slope of the curve of log $\frac{F_0-F}{F}$ versus log $\frac{1}{([Q]-\left(\frac{F_0-F}{F_0}\right)[P])}$, and the value of K_b is determined from its intercept.

If fluorescence quenching measurements are performed at different temperatures, the thermodynamic parameters can be obtained, allowing an understanding of the molecular forces driving the interaction process and providing information about possible structural changes in the interacting molecules owing to the binding process (Bujalowski and Jezewska, 2014). The most relevant parameters of a thermodynamic binding process are the ΔG°, ΔH°, and ΔS° of the system under standard conditions (1 mol/L of interacting molecules at 25 °C). The ΔG° values for the complex formation are determined directly from the K_b values using Eq. 3 (Nunes et al. 2017).

$$\Delta G° = -RTlnK_b, \quad (3)$$

where R is the universal gas constant (8.3145 J/mol/K), and T is the absolute temperature (K).

To calculate the $\Delta H°$ values, the linear adjustment of the lnK_b values vs. the inverse of each studied temperature can be applied to the Van 't Hoff equation (Eq. 4).

$$ln\frac{Kb_2}{Kb_1} = -\frac{\Delta H°}{R}(\frac{1}{T_2} - \frac{1}{T_1}). \quad (4)$$

If the relationship of lnK_b vs.1/T is nonlinear, these data can be polynomially fitted to Eq. (5), and thus, the $\Delta H°$ can be determined through Eq. 6.

$$ln\, K_b = a + b\left(\frac{1}{T}\right) + c\left(\frac{1}{T}\right)^2 + d\left(\frac{1}{T}\right)^3 \cdots, \quad (5)$$

$$\Delta H° = -R\left[b + 2c\left(\frac{1}{T}\right) + 3d\left(\frac{1}{T}\right)^2\right]. \quad (6)$$

The TΔS° of the complex formation can be calculated using the Gibbs fundamental equation (Eq. 7).

$$T\Delta S° = \Delta H° - \Delta G°. \quad (7)$$

Therefore, through a fluorescence quenching study, it is possible to obtain a complete binding and thermodynamic study of the intermolecular interactions between a fluorophore and a quencher molecule, such as the proteins α-am, α-La, and Lys and the quencher TA.

5. Experimental

5.1 Materials

TA (100 wt.%), α-am from Bacillus licheniformis (96 wt.%), bovine milk α-LA (≥ 85 wt.%), and Lys from chicken egg white (>90 wt.%) were purchased from Sigma-Aldrich (USA). Buffer solutions (pH 7.0 and 7.4) were prepared using dibasic sodium phosphate and mono-hydrated sodium phosphate purchased from Lab Impex Ltd. (USA).

5.2 Fluorescence Spectroscopy

Fluorescence measurements were performed using an LS55 fluorescence spectrophotometer (Perkin Elmer Inc., Waltham, MA, USA) equipped with a thermostat bath. The experiments with α-am and α-La were carried out at a physiological pH. A protein concentration of 3 μM (α-am, α-La, or Lys) was used with increasing concentrations of TA (from 0 to 4.29 μM) at different temperatures (293.15, 298.15, 303 .15, 308.15, and 313.15 K). The excitation wavelength was 295 nm, which is specific for Trp, and the slit widths for excitation and emission were set at 3.3 nm. Emission spectra were recorded in the range of 296–500 nm using a photomultiplier tube (PMT) voltage of 775 V and a scan rate of 700 nm/min. All experiments were performed in triplicate; data were analyzed using the Stern–Volmer, Van 't Hoff, and Gibbs equations. A schematic representation of the methodology is shown in Figure 7.

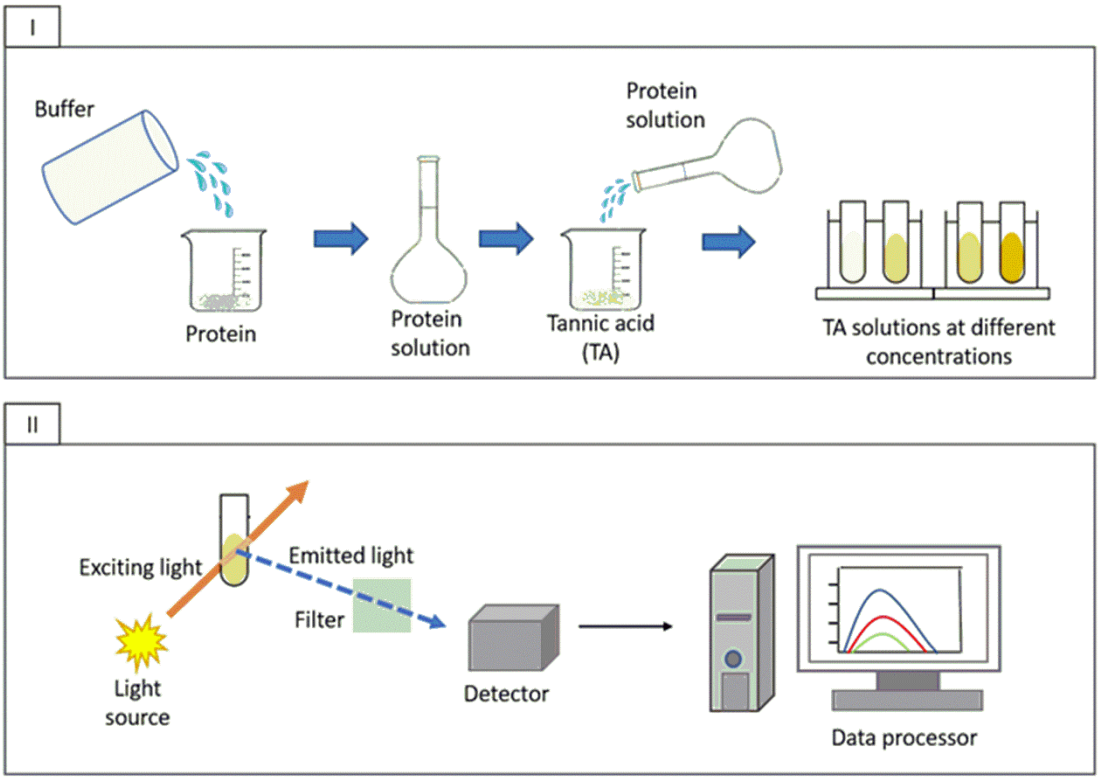

Figure 7. Schematic representation of the methodology; I: procedures for the preparation of proteins and TA solutions; II: schematic diagram of a measurement in a fluorescence spectrometer.

6. Analysis of the Fluorescence Suppression Mechanism of TA on α-am, α-LA, and Lys

The intrinsic fluorescence intensities of α-am, α-LA, and Lys with TA were analyzed to verify if TA molecules interact with the different proteins to form thermodynamically stable complexes. The fluorescence spectra of the three systems are shown in Figure 8.

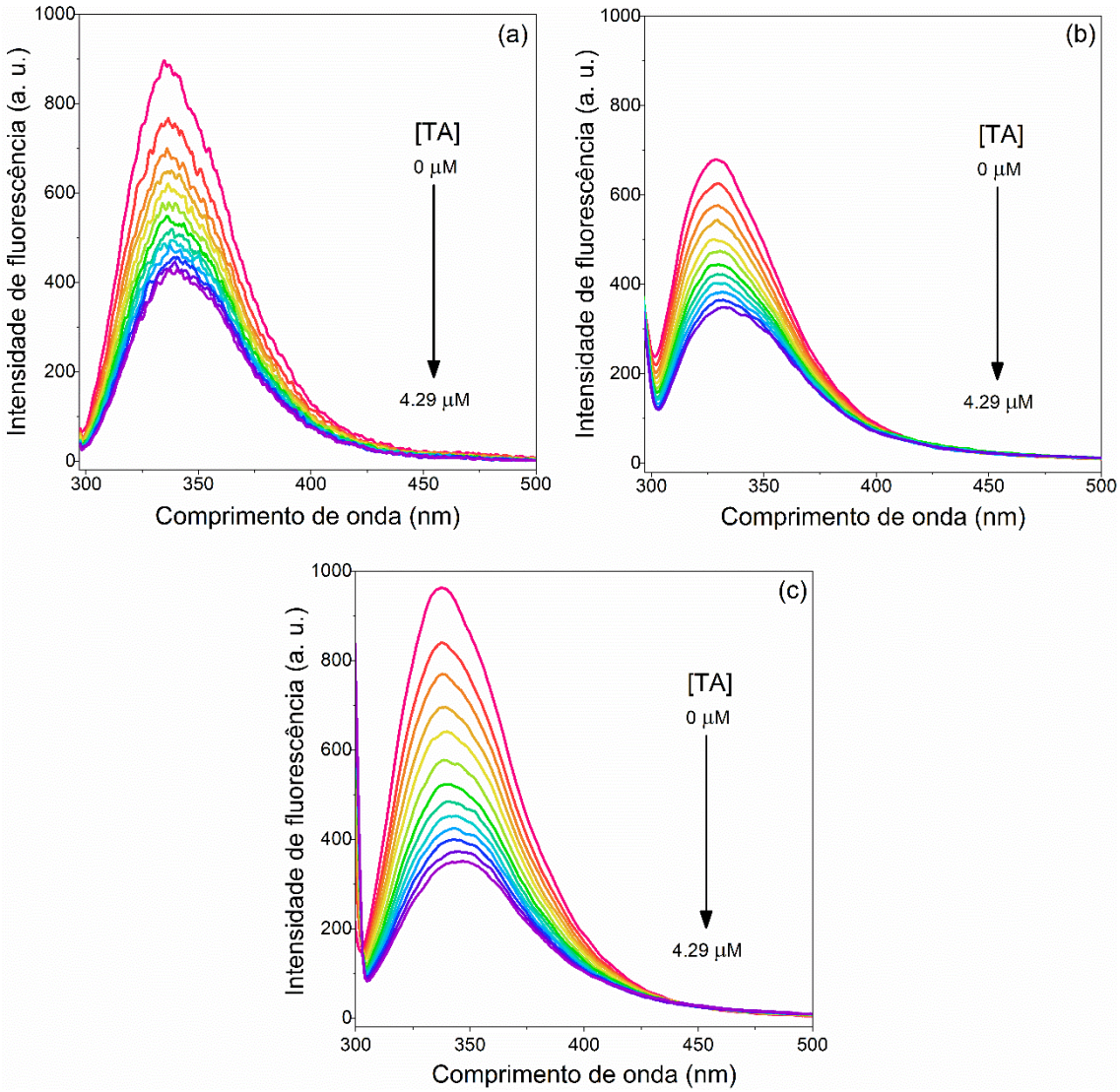

Figure 8. Fluorescence emission spectra of the α-am (a), α-La (b), and Lys (c) with increasing concentrations of TA at 298.15 K; the arrow indicates the increasing concentration of the TA (0 to 4.29 μM).

The presence of TA reduced the emitted fluorescence intensity of the Trp present in the chemical structure of the three protein molecules, i.e., the intrinsic fluorescence of α-am, α-La, and Lys was decreased. Fluorescence suppression can occur mainly because of two distinct mechanisms: i) static mechanism, in which the formation of a non-fluorescent thermodynamically stable complex occurs between the protein and the ligand, and ii) dynamic mechanism, in which collisions between the fluorophore and the quencher are responsible for quenching (Nunes et al., 2017).

The quenching mechanism can be characterized by evaluating the temperature dependence of the K_{sv}, that is, if K_{sv} decreases with increasing temperature, the suppression mechanism is classified as static; otherwise, it is dynamic. Therefore, the Stern–Volmer model (Eq. 8) was used to determine whether the mechanism was static or dynamic (Nunes et al., 2017).

$$\frac{F_0}{F} = 1 + K_q\tau_0[Q] = 1 + K_{SV}[Q], \quad (8)$$

where F_0 and F are the protein fluorescence intensities before and after the addition of the quencher (TA), respectively. [Q] is the total concentration of TA, K_{SV} is the Stern–Volmer constant, τ_0 is the lifetime of the protein without TA (approximately 10^{-8} s), and K_q is the biomolecular quenching constant. K_q was obtained from the relation $K_{sv} = K_q\tau_0$.

Figure 9 shows the Stern–Volmer plots for the fluorescence quenching of α-am, α-La, and Lys by TA at 298.15 K.

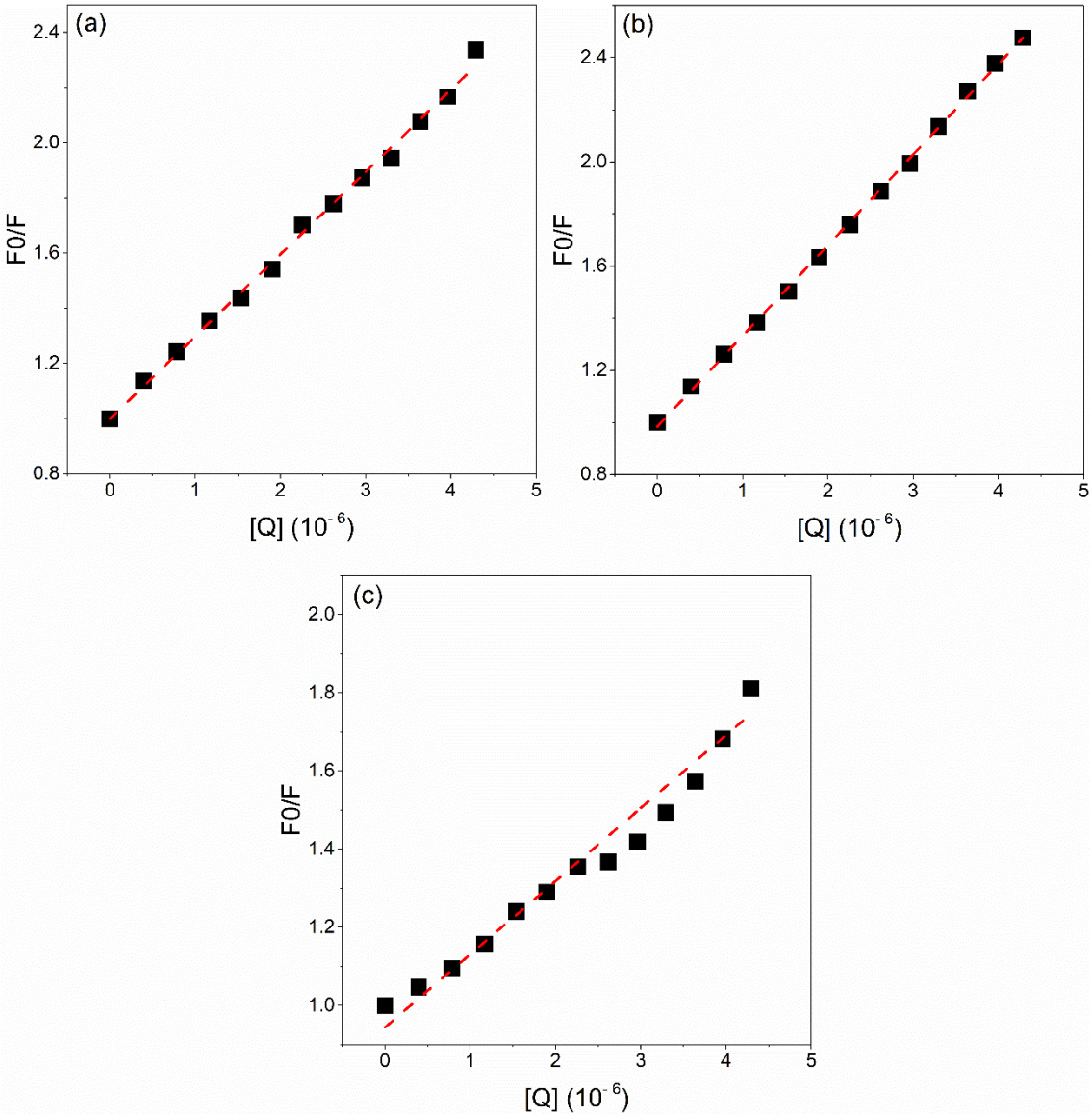

Figure 9. F_0/F versus [Q] plots for TA interacting with α-am (a), α-La (b), and Lys (c) at 298.15 K. The same behavior was observed at the other studied temperatures.

The Stern–Volmer plots for the interaction of TA with all analyzed proteins showed a positive linear profile with increasing quenching concentration (R_a^2 = 0.996, R_b^2 = 0.999, and R_c^2 = 0.930). This linear behavior confirms the presence of a single class of fluorophores (Trp residues in this case), which is equally accessed by the TA molecule (Lakowicz, 2006). From the slope of the curves shown in Figure 9, the K_{sv} values were obtained, and their temperature dependence is shown in Figure 10.

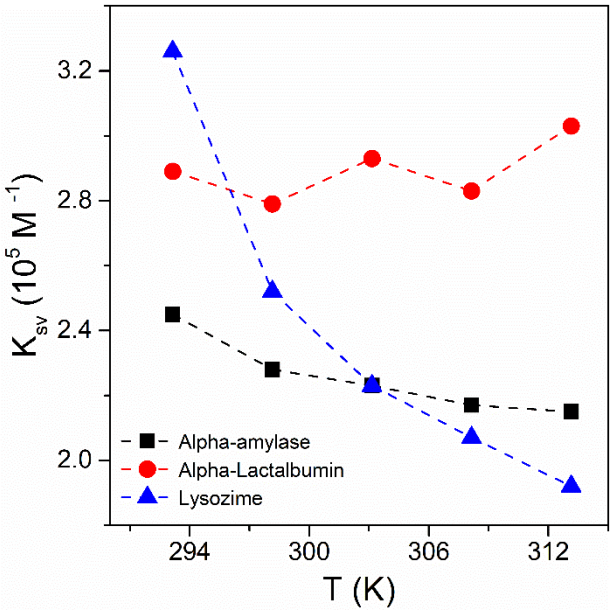

Figure 10. Temperature dependence of the K_{SV} values for the TA systems with α-am, α-La, or Lys.

Another method to identify the quenching mechanism is to analyze the value of K_q. That is, if the value is higher than 10^{10} L/mol/s, fluorescence suppression occurs owing to the complex formation (static suppression) (Rezende et al., 2019). Table 1 presents the K_q values of α-am, α-la, and Lys at the studied temperatures.

Table 1. The K_q values for α-am, α-la, and Lys at different temperatures.

T (K)	K_q ($10^{13} Lmol^{-1}s^{-1}$)		
	α-am	α-La	Lys
293.15	2.45	2.89	3.26
298.15	2.28	2.79	2.52
303.15	2.23	2.93	2.23
308.15	2.16	2.83	2.07
313.15	2.17	3.03	1.92

As shown in Figure 10, the K_{sv} values obtained for the α-am–TA and Lys–TA experiments decreased with increasing temperature, indicating that the fluorescence suppression of these proteins occurred predominantly through the static mechanism

with the formation of a complex with TA. Furthermore, the K_q values for the α-am and Lys were higher than the maximum K_q value for collisional suppression.

Although the K_{sv} values for the α-La–TA interaction did not decrease with increasing temperature, the K_q values were approximately 1000 times higher than the maximum collisional K_q, indicating the formation of a complex between TA and the protein.

When a thermodynamically stable complex was formed, the fluorescence measurement data were used to calculate the K_b and n of the complex formed through the logarithmic regression curve of Eq. 9, Figure 11 (REZENDE et al., 2019).

$$\log \frac{F_0 - F}{F} = n \log K_b - n \log \frac{1}{([Q] - \left(\frac{F_0 - F}{F_0}\right)[P])}, \quad (9)$$

where F_0 and F are the fluorescence intensities of the proteins before and after the addition of the inhibitor molecule, respectively, [Q] is the total concentration of TA, and [P] is the total concentration of the α-am, α-La, or Lys. The value of n corresponds to the slope of the curve of $\log \frac{F_0 - F}{F}$ versus $\log \frac{1}{([Q] - \left(\frac{F_0 - F}{F_0}\right)[P])}$, and the value of K_b is obtained from its interception.

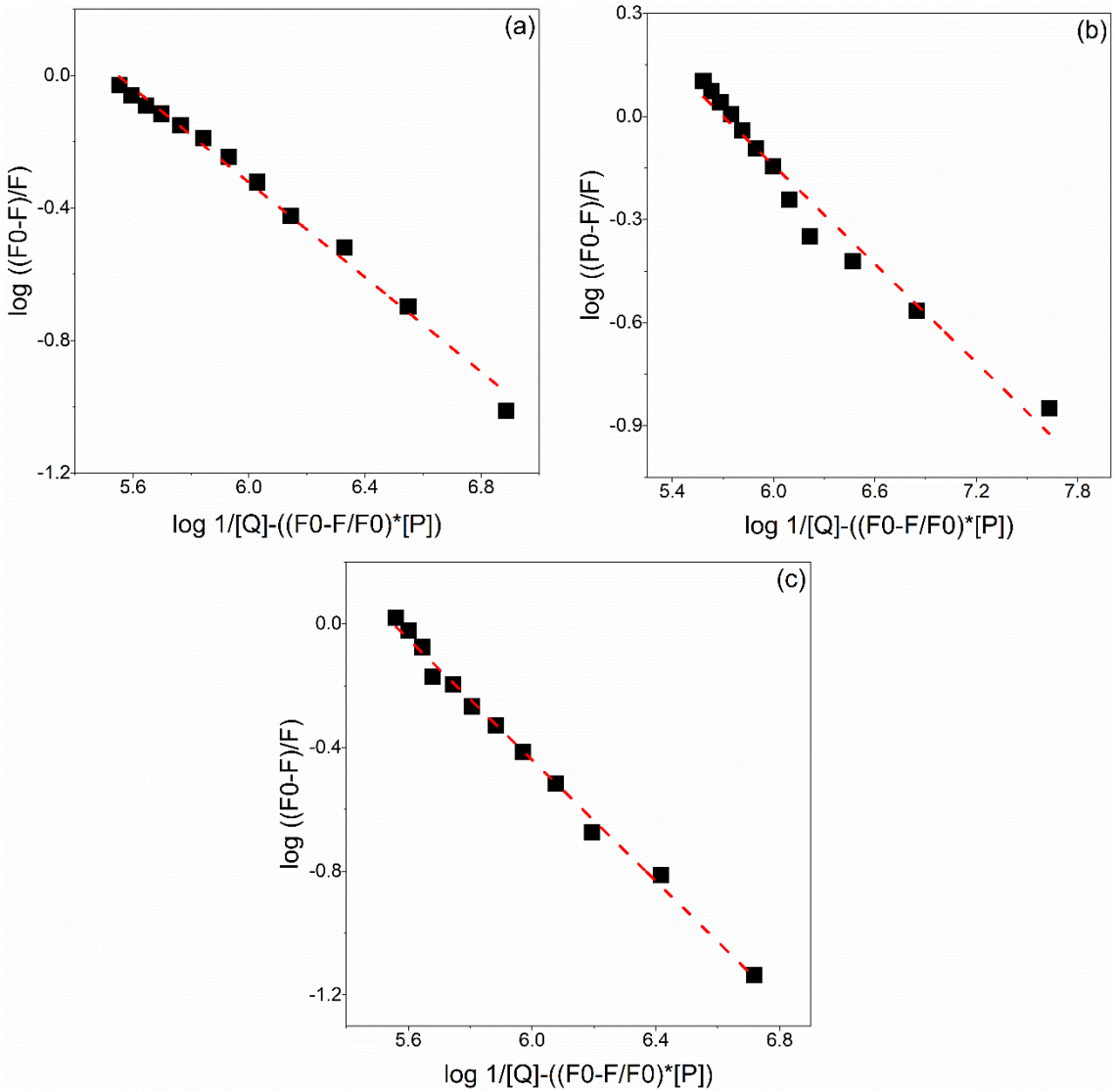

Figure 11. Graph representation of log $\frac{F_0-F}{F}$ versus log $\frac{1}{([Q]-\left(\frac{F_0-F}{F_0}\right)[P])}$ for TA interacting with α-am (a), α-La (b), and Lys (c) at 298.15 K. The same behavior was obtained at other studied temperatures.

The double logarithm regression curves for the interactions of TA with the α-am (R2 = 0.991), α-La (R2 = 0.969), and Lys (R2 = 0.994) were linear throughout the ligand concentration range. This linearity indicates the formation of stable complexes, thereby conferring reliability to the determination of the values of n and K_b from the slope and Y-axis intercept of the curves, respectively. The values of n for the three systems are listed in Table 2.

Table 2. *n* values of the formation of the TA complexes with α-am, α-La, and Lys at different temperatures.

T (K)	Stoichiometry (*n*)*		
	α-am–TA	α-La–TA	Lys–TA
293.15	0.43	0.65	0.75
298.15	0.53	0.54	0.90
303.15	0.49	0.66	0.81
308.15	0.49	0.64	0.92
313.15	0.56	0.62	0.70

*The R^2 values were higher than 0.98 at all temperatures of the three studied complexes.

The n values for the α-am–TA and α-La–TA complexes were approximately 0.5, and that of Lys–TA was approximately 1. That is, one TA molecule interacted with two binding sites of α-am and α-La (1:2), while one TA molecule interacted with one Lys binding site (1:1).

The temperature dependence of the K_b values of the complexes between TA and α-am, α-La, or Lys is shown in Figure 12.

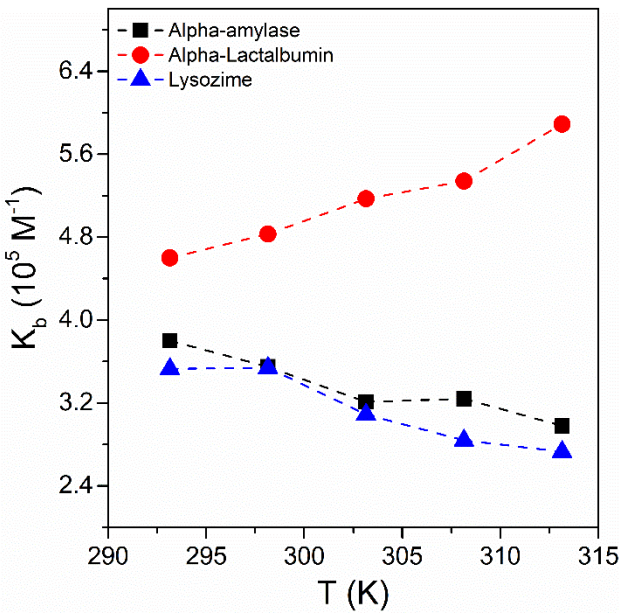

Figure 12. Temperature dependence of the K_b values of the TA complexes with α-am, α-La, or Lys.

The K_b values of the α-am and Lys complexes decreased with increasing temperatures. This behavior indicates that the formation of the complexes is an exothermic thermodynamic process; that is, as the temperature increased, relatively few α-am–TA and Lys–TA complexes were formed. In contrast, the K_b values for the α-La system increased by approximately 28% as the temperature increased, indicating that the increase in temperature favored the formation of the α-La–TA complexes (endothermic process).

7. Thermodynamic Analysis of the Formation of the α-am–TA, α-La–TA, and Lys–TA Complexes

Thermodynamic analysis was performed to understand the forces that drive the formation of the α-am–TA, α-La–TA, and Lys–TA complexes. The thermodynamic parameters (ΔG°, ΔH°, TΔS°, and standard heat capacity variation (ΔCp°)) were calculated as shown below.

The ΔG° values were directly calculated using Eq. 10. The ΔH° values were determined by plotting lnK_b versus 1/T (Van 't Hoff plot). Thereafter, a polynomial function was fitted to the Van 't Hoff data to determine the values of the constants a, b, and c (Eq. 11). Knowing these constants, the ΔH° values were determined using Eq. 12. Finally, the TΔS° values were obtained using the fundamental Gibbs equation (Eq. 13).

$$\Delta G° = -RT\ ln\ K_b, \tag{10}$$

$$lnK_b = a + b\left(\frac{1}{T}\right) + c\left(\frac{1}{T}\right)^2, \tag{11}$$

$$\Delta H^0 = -R\frac{dlnK_b}{d\left(\frac{1}{T}\right)} \rightarrow \Delta H^0 = -R\left[b + 2c\left(\frac{1}{T}\right)\right], \tag{12}$$

$$\Delta G° = \Delta H° - T\Delta S°. \tag{13}$$

ΔCp° was obtained from the slope of the ΔH° versus temperature graph according to the relationship expressed in Eq. 14.

$$\Delta Cp^0 = \frac{\partial \Delta H^0}{\partial T}. \quad (14)$$

The calculated thermodynamic parameters are presented in Tables 3, 4, and 5.

Table 3. Thermodynamic parameters of the α-am–TA complex formation.

T (K)	ΔH^0	ΔG^0	$\mathrm{T}\Delta S^0$	ΔCp^0
	kJ/mol			
293.15	−11.49	−31.31	19.82	
298.15	−10.12	−31.68	21.57	
303.15	−8.79	−31.96	23.17	0.26
308.15	−7.50	−32.51	25.01	
313.15	−6.26	−32.81	26.55	

Table 4. Thermodynamic parameters of the α-La–TA complex formation.

T (K)	ΔH^0	ΔG^0	$\mathrm{T}\Delta S^0$	ΔCp^0
	kJ/mol			
293.15	6.00	−31.78	37.78	
298.15	7.62	−32.44	40.06	
303.15	9.18	−33.16	42.34	0.30
308.15	10.69	−33.79	44.47	
313.15	12.15	−34.59	46.54	

Table 5. Thermodynamic parameters of the Lys–TA complex formation.

T (K)	ΔH^0	ΔG^0	$\mathrm{T}\Delta S^0$	ΔCp^0
	kJ/mol			
293.15	−8.54	−31.13	22.59	
298.15	−9.94	−31.67	21.73	
303.15	−11.29	−31.86	20.57	−0.27
308.15	−12.61	−32.17	19.56	
313.15	−13.88	−32.59	18.71	

For the three studied complexes, the ΔG° values were negative, indicating that, in the $Protein + TA \leftrightharpoons Protein - TA$ thermodynamic equilibrium, more complexes were formed with the free molecules. The analysis of the enthalpic and entropic components of ΔG° allowed us to understand which molecular processes predominated during the complex formation.

The ΔH° is related to the energy expenditure for the desolvation process of proteins and TA ($\Delta H^0_{dess} > 0$) at the enthalpy cost of the conformational changes of site adjustment ($\Delta H^0_{conf} > 0$) and the energy released from the direct interactions formed between the desolvated amino acid residues of the α-am and TA ($\Delta H^0_{int\ \mathrm{Protein-TA}} < 0$). A similar analysis was performed for ($T\Delta S^0$): $T\Delta S^0 = T\Delta S^0_{dess} + T\Delta S^0_{conf} + T\Delta S^0_{int\ \mathrm{Protein-TA}}$.

As shown in Table 3, the ΔH° values for the formation of the α-am–TA complex are negative, indicating that the energy released from the specific interactions between the non-solvated protein site and ligand had a relatively high contribution to the enthalpy change of the system. Additionally, based on the magnitude and signal of the ΔH°(α-am–TA), the [α-am–TA]o complex formation may be due to the hydrophilic interactions owing to hydrogen bonds (HBI). The ΔH°(α-am–TA) values became less negative with increasing temperature (from -11.49 to $-6.26\ kJmol^{-1}$). This was probably because the HBI is an oriented and cooperative interaction, and to have more optimized HBI interactions, the TA OH group should be oriented in relation to the (–COOH) or (–NH2) groups of the amino acid segment. At relatively high temperatures, the potential rotation barrier of a single O–C bond binding the central glucose unit to gallic acid molecules was of the same order of magnitude as 3/2 KT. Under these thermodynamic conditions, the almost free O–C bond rotation made the HB group orientation more difficult, and consequently, the formation of HBI was difficult, releasing less energy during the α-am–TA interaction. The non-dominant contribution of the $\Delta H^0_{dess} + \Delta H^0_{conf}$ values for the ΔH° magnitude suggests that the α-m–TA interaction occurred through a small extension desolvation and protein site conformation change processes, releasing a small number of water molecules and causing a small protein site conformation change. Regarding the entropic terms, the values of the TΔS° were positive, increasing with temperature enhancement (from 19.82 to $25.55\ kJmol^{-1}$). This indicates that, although the desolvation and conformation change processes of the interacting molecules do not make the main contribution to the ΔH° values, they

determine the TΔS° magnitude. The effect of the increase in temperature on the TΔS° values should be attributed to the increase in protein site flexibility observed at relatively high temperatures, making it possible to extend the protein site conformation to the conformation of the TA molecule.

The values of the enthalpic (from 6.00 to $12.15\ kJmol^{-1}$) and entropic (from 37.78 to $46.54\ kJmol^{-1}$) components for the α-La–TA interaction, as shown in Table 4, were positive and increased with increasing temperature. This demonstrated that the main force involved in the formation of the thermodynamically stable a-La–TA complex was the hydrophobic interactions. It is well known that the hydrophobic interactions are promoted by the release of water molecules from the solvation shell of the hydrophobic surface of the interacting molecules. As these water molecules are more structured and produce more intense HBI, their release into the bulk implies the absorption of enthalpic energy ($\Delta H^0_{dess} > 0$), as well as a system entropic gain ($\Delta S^0_{dess} > 0$). Additionally, as previously discussed, the increase in the temperature increases the flexibility of the interacting protein site, favoring the inclusion of TA molecules more deeply and in more hydrophobic regions of the α-La, resulting in increased energy expenditure. Similar behavior was observed for the α-La and quinoline yellow food additive coloring ($\Delta H^0_{298.15K} = 18.79\ kcalmol^{-1}$ and $\Delta S^0_{298.15K} = 83.71 \frac{kcal}{} mol^{-1}.K^{-1}$). Furthermore, in this study, the increase in temperature favored the formation of the complexes (K_b ranging from 0.091 to $0.955\ 10^{-5} Lmol^{-1}$); however, the stoichiometry was 1:1 (Al-Shabib et al., 2020).

The Lys–TA complex presented negative values for the enthalpic components and positive values for the entropic components. However, the values of ΔH° (-8.54 para $-13.88\ kJmol^{-1}$) and TΔS° (22.59 para $18.17\ kJmol^{-1}$) decreased with increasing temperature. These results indicate that the process of the formation of the Lys–TA complex was enthalpy- and entropy-governed. Further, with an increase in the average molecular kinetic energy, there was an increased interaction of TA within the Lys, which allowed the formation of new specific interactions, releasing more enthalpic energy and increasing the entropy of the system. Su et al. (2019) carried out a thermodynamic study of the Lys–TA complex using the FS technique at pH 6.0 at temperatures 298.15 and 310.15, and they obtained similar stoichiometric values (1:1). However, the enthalpy and entropy values were different ($\Delta H^0 = 4.954\ kJmol^{-1}$ and $\Delta S^0_{298.15K} = 0.114\ kJ.K^{-1}$). Additionally, the influence of temperature on the formation

of the complexes was not analyzed because the experiment was carried out at only two temperatures. The results presented in the present work demonstrate that temperature significantly influences the formation of the Lys–TA complex, demonstrating the importance of thermodynamic studies with a relatively high number of temperatures.

ΔCp° is related to the relative distribution of energy transferred to the system in the form of potential components (chemical bonds, intermolecular interactions, etc.) and kinetics (translation, rotation, vibration, etc.). Hence, this parameter reflects the difference in the intensity of the intermolecular interactions in the complex compared to those in the free molecules ($\Delta Cp^0 = Cp^0_{\text{Protein-TA}} - (Cp^0_{\text{Protein}} + Cp^0_{TA})$).

The positive values of ΔCp° for α-am (0.26 kJ/mol/K) and α-La (0.30 kJ/mol/K) indicated that the number and/or intensity of interactions in the free molecules were inferior to the new interactions formed in the complexes. For the Lys–TA, the value of ΔCp° was negative (−0.27 kJ/mol/K), i.e., the number/intensity of the interactions of the Lys–TA complex was higher than that of the interactions within the protein and between the molecules of water and Lys and/or TA.

8. Conclusion

TA forms thermodynamically stable complexes with Lys, α-La, or α-am proteins. The thermodynamic properties of the complex formation in general, and specifically, the driving force of the TA–protein interaction, were dependent on the chemical structure of the biopolymers. The α-am–TA complex was formed by hydrophilic interactions, mainly caused by the formation of hydrogen bonds between the TA molecules and the amino acid residues of α-am. For the a-La–TA complexes, hydrophobic interactions led to strong interactions between the two molecules. Finally, for the Lys–TA complex, both hydrophilic and hydrophobic interactions contributed to the stabilization of the supramolecular complex. These results demonstrate that TA can perform the molecular recognition process of both hydrophilic and hydrophobic sites; thus, the TA molecule can be used as a "link" in the construction of supramolecular structures using proteins as building units.

Acknowledgments

The authors thank the Coordenação de Aperfeiçoamento de Pessoal de Nível Superior (CAPES), Conselho Nacional de Desenvolvimento Científico e Tecnológico (CNPq), and Fundação de Apoio à Pesquisa de Minas Gerais (FAPEMIG) for the financial support.

9. References

Abbas, M. M., YOUNIS, K. M., & HUSSAIN, W. S. (2021). Impact of medicinal plants on corona pandemic. Plant Cell Biotechnology and Molecular Biology, 22(19–20), 62–72.

Abdelli, I., Benariba, N., Adjdir, S., Fekhikher, Z., Daoud, I., Terki, M., Benramdane, H., & Ghalem, S. (2021). In silico evaluation of phenolic compounds as inhibitors of A-amylase and A-glucosidase. Journal of Biomolecular Structure and Dynamics, 39(3), 816–822. https://doi.org/10.1080/07391102.2020.1718553

Al-Shabib, N. A., Khan, J. M., Malik, A., Rehman, M. T., AlAjmi, M. F., Husain, F. M., Ahmed, M. Z., & Alamery, S. F. (2020). Molecular interactions of food additive dye quinoline yellow (Qy) with alpha-lactalbumin: Spectroscopic and computational studies. Journal of Molecular Liquids, 311, 113215. https://doi.org/10.1016/j.molliq.2020.113215

Avwioroko, O. J., Anigboro, A. A., Atanu, F. O., Otuechere, C. A., Alfred, M. O., Abugo, J. N., & Omorogie, M. O. (2020). Investigation of the binding interaction of α-amylase with Chrysophyllum albidum seed extract and its silver nanoparticles: A multi-spectroscopic approach. Chemical Data Collections, 29, 100517. https://doi.org/10.1016/j.cdc.2020.100517

Belhaoues, S., Amri, S., & Bensouilah, M. (2020). Major phenolic compounds, antioxidant and antibacterial activities of Anthemis praecox Link aerial parts. South African Journal of Botany, 131, 200–205. https://doi.org/10.1016/j.sajb.2020.02.018

Bhargava, N., Mor, R. S., Kumar, K., & Sharanagat, V. S. (2021). Advances in application of ultrasound in food processing: A review. Ultrasonics Sonochemistry, 70, 105293. https://doi.org/10.1016/j.ultsonch.2020.105293

Brew, K. (2011). Milk Proteins | α-Lactalbumin. In Encyclopedia of Dairy Sciences (pp. 780–786). Elsevier. https://doi.org/10.1016/B978-0-12-374407-4.00432-5

Cao, D., Wu, H., Li, Q., Sun, Y., Liu, T., Fei, J., Zhao, Y., Wu, S., Hu, X., & Li, N. (2015). Expression of recombinant human lysozyme in egg whites of transgenic hens. PLoS ONE, 10(2), 1–15. https://doi.org/10.1371/journal.pone.0118626

Chen, C., Shi, K., Qin, X., Zhang, H., Chen, H., Hayes, D. G., Wu, Q., Hu, Z., & Liu, G. (2021). Effect of interactions between glycosylated protein and tannic acid on the physicochemical stability of Pickering emulsions. Lwt, 152(68), 112383. https://doi.org/10.1016/j.lwt.2021.112383

Company, P. (1975). SEPARATION OF HUMAN a-AMYLASE ISOZYMES BY ELECTRO- FOCUSING AND THEIR IMMUNOLOGICAL PROPERTIES.

Das, S., Ghosh, P., Koley, S., & Singha Roy, A. (2018). Binding of naringin and naringenin with hen egg white lysozyme: A spectroscopic investigation and molecular docking study. In Spectrochimica Acta - Part A: Molecular and Biomolecular Spectroscopy (Vol. 192). Elsevier B.V. https://doi.org/10.1016/j.saa.2017.11.015

De Wit, J. N. (1998). Nutritional and Functional Characteristics of Whey Proteins in Food Products. Journal of Dairy Science, 81(3), 597–608. https://doi.org/10.3168/jds.S0022-0302(98)75613-9

Delavari, B., Saboury, A. A., Atri, M. S., Ghasemi, A., Bigdeli, B., Khammari, A., Maghami, P., Moosavi-Movahedi, A. A., Haertlé, T., & Goliaei, B. (2015). Alpha-lactalbumin : A new carrier for vitamin D3 food enrichment. Food Hydrocolloids, 45, 124–131. https://doi.org/10.1016/j.foodhyd.2014.10.017

Duy, C., & Fitter, J. (2006). How aggregation and conformational scrambling of unfolded states govern fluorescence emission spectra. Biophysical Journal, 90(10), 3704–3711. https://doi.org/10.1529/biophysj.105.078980

Esobi, I. C., Lasode, M. K., & Barriguete, M. O. F. (2020). The Impact of COVID-19 on Healthy Eating Habits. Journal of Clinical Nutrition and Health, 1(1), 1–2. https://doi.org/10.47755/jcnh.1000105

Faber, C., Hobley, T. J., Mollerup, J., Thomas, O. R. T., & Kaasgaard, S. G. (2007). Study of the Solubility of a Modified Bacillus licheniformis r -Amylase around the Isoelectric Point. 707–713.

Fleming, A. (1920). Downloaded from https://royalsocietypublishing.org/ on 01 August 2021 On a Remarkable Bacteriolytic Element found Downloaded from https://royalsocietypublishing.org/ on 01 August 2021.

Forsythe, E. L., Snell, E. H., Malone, C. C., & Pusey, M. L. (1999). Crystallization of chicken egg white lysozyme from assorted sulfate salts. Journal of Crystal Growth, 196(2–4), 332–343. https://doi.org/10.1016/S0022-0248(98)00843-4

Hamdani, A. M., Wani, I. A., Bhat, N. A., & Siddiqi, R. A. (2018). Effect of guar gum conjugation on functional, antioxidant and antimicrobial activity of egg white lysozyme. Food Chemistry, 240(August 2017), 1201–1209. https://doi.org/10.1016/j.foodchem.2017.08.060

Hui, X., Wu, G., Han, D., Stipkovits, L., Wu, X., Tang, S., Brennan, M. A., & Brennan, C. S. (2020). The effects of bioactive compounds from blueberry and blackcurrant powders on the inhibitory activities of oat bran pastes against α-amylase and α-glucosidase linked to type 2 diabetes. Food Research International, 138(PA), 109756. https://doi.org/10.1016/j.foodres.2020.109756

Ji, Y., Liu, D., Zhao, J., Zhao, J., Li, H., Li, L., Zhang, H., & Wang, H. (2021). α -glucosidase and α -amylase. 145(April).

Kaczmarek, B. (2020). Tannic acid with antiviral and antibacterial activity as a promising component of biomaterials-A minireview. Materials, 13(14). https://doi.org/10.3390/ma13143224

Kamau, S. M., Cheison, S. C., Chen, W., Liu, X. M., & Lu, R. R. (2010). Alpha-lactalbumin: Its production technologies and bioactive peptides. Comprehensive Reviews in Food Science and Food Safety, 9(2), 197–212. https://doi.org/10.1111/j.1541-4337.2009.00100.x

Khan, I., Dowarha, D., Katte, R., Chou, R., & Filipe, A. (2022). Lisozima como agente antiproliferativo para bloquear a interação entre S100A6 e o domínio RAGE V. 1–9.

Kim, T. J., Silva, J. L., Kim, M. K., & Jung, Y. S. (2010). Enhanced antioxidant capacity and antimicrobial activity of tannic acid by thermal processing. Food Chemistry, 118(3), 740–746. https://doi.org/10.1016/j.foodchem.2009.05.060

Lakowicz, J. R. (2006). Principles of Fluorescence Spectroscopy (Trird edit). https://doi.org/10.1007/978-0-387-46312-4

Leśnierowski, G., & Yang, T. (2021). Lysozyme and its modified forms: A critical appraisal of selected properties and potential. Trends in Food Science and Technology, 107(August 2020), 333–342. https://doi.org/10.1016/j.tifs.2020.11.004

Lesschaeve, I., & Noble, A. C. (2005). Polyphenols: factors influencing their sensory properties and their effects on food and beverage preferences. The American

Journal of Clinical Nutrition, 81(1 Suppl), 330–335. https://doi.org/10.1093/ajcn/81.1.330s

Lou, W., Chen, Y., Ma, H., Liang, G., & Liu, B. (2018). Antioxidant and α-amylase inhibitory activities of tannic acid. Journal of Food Science and Technology, 55(9), 3640–3646. https://doi.org/10.1007/s13197-018-3292-x

Magalhães, O. F., De Paula, H. M. C., Rezende, J. de P., Coelho, Y. L., Mendes, T. A. de O., Da Silva, L. H. M., & Pires, A. C. dos S. (2021). Energetic and molecular dynamic characterization of lysozyme/β-carotene interaction. Journal of Molecular Liquids, 337, 1–10. https://doi.org/10.1016/j.molliq.2021.116404

Mohammadi, F., & Moeeni, M. (2015a). Analysis of binding interaction of genistein and kaempferol with bovine α-lactalbumin. Journal of Functional Foods, 12, 458–467. https://doi.org/10.1016/j.jff.2014.12.012

Mohammadi, F., & Moeeni, M. (2015b). Study on the interactions of trans-resveratrol and curcumin with bovine α-lactalbumin by spectroscopic analysis and molecular docking. Materials Science and Engineering: C, 50, 358–366. https://doi.org/10.1016/j.msec.2015.02.007

Nguyen, V. B., Nguyen, A. D., Nguyen, Q. V., & Wang, S. L. (2017). Porcine pancreatic α-amylase inhibitors from Euonymus laxiflorus Champ. Research on Chemical Intermediates, 43(1), 259–269. https://doi.org/10.1007/s11164-016-2619-3

Nunes, Natália M., Coelho, Y. L., Castro, J. S., Vidigal, M. C. T. R., Mendes, T. A. O., da Silva, L. H. M., & Pires, A. C. S. (2020). Naringenin-lactoferrin binding: Impact on naringenin bitterness and thermodynamic characterization of the complex. Food Chemistry, 331(June), 127337. https://doi.org/10.1016/j.foodchem.2020.127337

Nunes, Natália Moreira, Pacheco, A. F. C., Agudelo, Á. J. P., da Silva, L. H. M., Pinto, M. S., Hespanhol, M. do C., & Pires, A. C. dos S. (2017). Interaction of cinnamic acid and methyl cinnamate with bovine serum albumin: A thermodynamic approach. Food Chemistry, 237, 525–531. https://doi.org/10.1016/J.FOODCHEM.2017.05.131

Ong, J. N., Hackett, D. A., & Chow, C. (2017). Sleep quality and duration following evening intake of alpha-lactalbumin : a pilot study. Biological Rhythm Research, 1016(April), 0. https://doi.org/10.1080/09291016.2016.1275398

Permyakov, E. A., & Berliner, L. J. (2000). α-Lactalbumin: structure and function. FEBS Letters, 473(3), 269–274. https://doi.org/10.1016/S0014-5793(00)01546-5

Perusko, M., Al-Hanish, A., Mihailovic, J., Minic, S., Trifunovic, S., Prodic, I., & Cirkovic Velickovic, T. (2017). Antioxidative capacity and binding affinity of the complex of green tea catechin and beta-lactoglobulin glycated by the Maillard reaction. Food Chemistry, 232, 744–752. https://doi.org/10.1016/j.foodchem.2017.04.074

Rezende, J. de P., Coelho, Y. L., de Paula, H. M. C., da Silva, L. H. M., & Pires, A. C. dos S. (2020). Temperature modulation of lutein-lysozyme hydrophobic-hydrophilic interaction balance. Journal of Molecular Liquids, 316, 113887. https://doi.org/10.1016/j.molliq.2020.113887

Rezende, J. de P., Hudson, E. A., de Paula, H. M. C., Coelho, Y. L., da Silva, L. H. M., & Pires, A. C. dos S. (2019). Thermodynamic and kinetic study of epigallocatechin-3-gallate-bovine lactoferrin complex formation determined by surface plasmon resonance (SPR): A comparative study with fluorescence spectroscopy. Food Hydrocolloids, 95, 526–532. https://doi.org/10.1016/j.foodhyd.2019.04.065

Romano, A., Lajterer, C., Shpigelman, A., & Lesmes, U. (2021). Bovine alpha-lactalbumin assemblies with capsaicin : Formation , interactions , loading and physiochemical characterization. Food Chemistry, 352(February), 129306. https://doi.org/10.1016/j.foodchem.2021.129306

Santa Rosa, L. N., Rezende, J. de P., Coelho, Y. L., Mendes, T. A. O., da Silva, L. H. M., & Pires, A. C. dos S. (2021). B-Lactoglobulin Conformation Influences Its Interaction With Caffeine. Food Bioscience, 44(July). https://doi.org/10.1016/j.fbio.2021.101418

Seres, D. S., & Coates, P. M. (2021). Comment on “Western Dietary Pattern Antioxidant Intakes and Oxidative Stress: Importance during the SARS-CoV-2/COVID-19 Pandemic.” Advances in Nutrition, 12(3), 1045–1046. https://doi.org/10.1093/advances/nmab030

Soares, S., Brandão, E., Guerreiro, C., Soares, S., Mateus, N., & De Freitas, V. (2020). Tannins in food: Insights into the molecular perception of astringency and bitter taste. Molecules, 25(11), 1–26. https://doi.org/10.3390/molecules25112590

Su, J., Sun, Y., Li, Z., Chen, Y., Ding, B., & Sun, W. (2019). Effect of tannic acid on lysozyme activity through intermolecular noncovalent binding. Journal of Agriculture and Food Research, 1(October), 100004. https://doi.org/10.1016/j.jafr.2019.100004

Sun, L., Chen, W., Meng, Y., Yang, X., Yuan, L., & Guo, Y. (2016). Interactions between polyphenols in thinned young apples and porcine pancreatic α-amylase:

Inhibition, detailed kinetics and fluorescence quenching. Food Chemistry, 208, 51–60. https://doi.org/10.1016/j.foodchem.2016.03.093

Tagashira, A., Nishi, K., Matsumoto, S., & Sugahara, T. (2018). Anti-inflammatory effect of lysozyme from hen egg white on mouse peritoneal macrophages. Cytotechnology, 70(3), 929–938. https://doi.org/10.1007/s10616-017-0184-2

Vilcacundo, R., Méndez, P., Reyes, W., Romero, H., Pinto, A., & Carrillo, W. (2018). Antibacterial activity of hen egg white lysozyme denatured by thermal and chemical treatments. Scientia Pharmaceutica, 86(4), 1–17. https://doi.org/10.3390/scipharm86040048

Violet, M., & Meunier, J. (1989). Kinetic study of the irreversible thermal denaturation of Bacillus licheniformis a-amylase. 263, 665–670.

Wu, Tiantian, Jiang, Q., Wu, D., Hu, Y., Chen, S., Ding, T., Ye, X., Liu, D., & Chen, J. (2019). What is new in lysozyme research and its application in food industry? A review. Food Chemistry, 274(September 2018), 698–709. https://doi.org/10.1016/j.foodchem.2018.09.017

Wu, Tingting, Zhou, X., Deng, Y., Jing, Q., Li, M., & Yuan, L. (2011). In vitro studies of Gynura divaricata (L.) DC extracts as inhibitors of key enzymes relevant for type 2 diabetes and hypertension. Journal of Ethnopharmacology, 136(2), 305–308. https://doi.org/10.1016/j.jep.2011.04.059

Yang, B., Wang, J., Tang, B., Liu, Y., Guo, C., Yang, P., Yu, T., Li, R., Zhao, J., Zhang, L., Dai, Y., & Li, N. (2011). Characterization of bioactive recombinant human lysozyme expressed in milk of cloned transgenic cattle. PLoS ONE, 6(3), 1–10. https://doi.org/10.1371/journal.pone.0017593

CAPÍTULO 2 – Efeito dos níveis de hidrofobicidade dos flavonoides na cinética e termodinâmica de suas interações com a alfa-lactoalbumina bovina

RESUMO

Os efeitos da temperatura e hidrofobicidade da naringina (NR) e naringenina (NG) em suas interações com α-lactalbumina (αLA) foram investigados analisando a termodinâmica e cinética das interações usando a técnica de ressonância plasmônica de superfície. O docking molecular foi realizado para avaliar os mecanismos moleculares das interações NG/NR–αLA. A constante de taxa de associação entre αLA e NR foi aproximadamente três vezes maior do que entre αLA e NG, e a constante de taxa de dissociação foi menor para αLA–NG do que para αLA–NR em todas as temperaturas avaliadas. O processo de formação de αLA–NG foram predominantemente entrópicos devido ao processo de dessolvatação para acessar sítios hidrofóbicos. A presença do grupo glicosídeo em NR promoveu interações hidrofílicas. O melhor modelo de ligação produzido por docking molecular sugeriu que ambas as moléculas se ligam à mesma cavidade proteica.

Palavras-chave: Interação proteína-flavonóide; ressonância plasmônica de superfície, docking molecular.

CHAPTER 2 – Effect of hydrophobicity level of flavonoids on the kinetics and thermodynamics of their interactions with bovine alpha-lactalbumin

ABSTRACT

The effects of the temperature and hydrophobicity of naringin (NR) and naringenin (NG) on their interactions with α-lactalbumin (αLA) were investigated by analyzing the thermodynamics and kinetics of the interactions using the surface plasmon resonance technique. Molecular docking was performed to assess the molecular mechanisms of the NG/NR–αLA interactions. The association rate constant between αLA and NR was approximately three-fold higher than that between αLA and NG, and the dissociation rate constant was lower for the αLA–NG than for αLA–NR at all temperatures evaluated. The formation process of αLA–NG was predominantly entropic because of the desolvation process to access hydrophobic sites. Contrarily, the presence of the glycoside group in NR promoted hydrophilic interactions. The best binding model produced by molecular docking suggested that both molecules bind to the same protein cavity.

Keywords: protein-flavonoid binding; surface plasmon resonance, molecular docking.

1. Introduction

There are few studies on the molecular dynamics of supramolecular complexes formed between proteins and bioactive molecules, which makes it difficult to establish the formation mechanisms of these complexes. In addition, some recent studies have shown that even small changes in the chemical structure of interacting molecules can modify the kinetics and thermodynamics of complex formation (Paiva et al., 2020; Rezende et al., 2020). Understanding these factors may present a competitive advantage in the application of protein–bioactive-molecule complexes in/under different matrices and thermodynamic conditions.

Surface plasmon resonance (SPR) is an interesting technique for investigating intermolecular interactions because it allows for qualitative and quantitative label-free detection, uses small amounts of reagents, and reuses the sensor chips (Rezende et al., 2020b). In addition, it allows for an evaluation of the kinetic and thermodynamic parameters of the connection, as well as a direct and real-time monitoring (HUDSON et al., 2019). Therefore, SPR can be utilized to analyze the kinetics and thermodynamics of complex formation between the α-lactalbumin protein (αLA) and naringin (NR) and naringenin (NG) molecules.

NG (Fig. S1) is a flavonoid with a molar mass of 272.2 g/mol and is found mainly in citrus fruits (particularly grapefruit); it is responsible for the bitter taste of these fruits. Notably, NG has three hydroxyl groups in its structure. NR (Fig. S1) has a molar mass of 580.4 g / mol, and its chemical structure includes a molecule of NG as one of the components (Alam et al., 2014; Nunes et al., 2020). Both NR and NG are strong antioxidants and anti-inflammatory agents, which have several nutraceutical effects, including protection against cardiovascular and neurodegenerative diseases, and antidiabetic effects (ADEBIYI; ADEBIYI; OWIRA, 2016; AL-DOSARI et al., 2017; HEIDARY MOGHADDAM et al., 2020; HILAIRE et al., 2017). However, the low solubility of these molecules in water environments limits their therapeutic applications (Nunes et al., 2020).

The formation of nanocomplexes between NR or NG and milk proteins has been studied as an alternative method for transporting these flavonoids and improving their bioavailability. For example, beta-casein (β-Cas) can form complexes with both NR (PACHECO et al., 2020) and NG (LI et al., 2019). The β-Cas–NR ($\Delta G^{\circ}_{293\,K} = -23.67\ kJ\ mol^{-1}$, $\Delta H^{\circ}_{293\,K} = 107.43\ kJ\ mol^{-1}$, and $T\Delta S^{\circ}_{293\,K} = 131.09\ kJ\ mol^{-1}$) and

β-Cas–NG studies ($\Delta G^{\circ}_{298\,K} = -31.42\ kJ\ mol^{-1}$, $\Delta H^{\circ}_{298\,K} = 17.62\ kJ\ mol^{-1}$, and $\Delta S^{\circ}_{298\,K} = 46.31\ J\ mol^{-1}K^{-1}$) highlighted the predominance of hydrophobic interactions in the formation of complexes involving flexible proteins. Regarding whey proteins, lactoferrin (LF) also forms complexes with NR (Nunes et al., 2019), and NG (Nunes et al., 2020) beta-lactoglobulin (βLG) complexed with NG (GHOLAMI; BORDBAR, 2014). The formation of the LF–NG complex ($\Delta G^{\circ}_{298\,K} = -33.42\ kJ\ mol^{-1}$, $\Delta H^{\circ}_{298\,K} = -2.61\ kJ\ mol^{-1}$, and $T\Delta S^{\circ}_{298\,K} = 30.81\ kJ\ mol^{-1}$) is mainly driven by an increase in entropy, while that of LF–NR is entropically driven up to 296 K ($\Delta G^{\circ}_{293\,K} = -28.78\ kJ\ mol^{-1}$, $\Delta H^{\circ}_{293\,K} = 68.79\ kJ\ mol^{-1}$, and $T\Delta S^{\circ}_{293\,K} = 97.57\ kJ\ mol^{-1}$) and enthalpically driven above 296 K ($\Delta G^{\circ}_{297\,K} = -29.30\ kJ\ mol^{-1}$, $\Delta H^{\circ}_{297\,K} = -32.76\ kJ\ mol^{-1}$, and $T\Delta S^{\circ}_{297\,K} = -3.46\ kJ\ mol^{-1}$). For βLG–NG, a thermodynamic study has not been performed.

Other milk proteins may have the potential to interact with these molecules of interest in food, pharmaceuticals, and cosmetics, among others. αLA is the second-largest whey protein. Therefore, its bioavailability is comparable to that of βLG, and it is considered less allergenic (COUTO et al., 2012). It has a molar mass of approximately 14.2 kDa and an isoelectric point of approximately 4.5. Further, αLA contains high proportions of cysteine, tryptophan, and branched amino acids, affording a high capacity to bind to various molecules, including phenolic compounds (AL-SHABIB et al., 2020). Mohammadi and Moeeni et al. (2015b) (2015a) found through fluorescence spectroscopy that at pH 7.4 and temperatures ranging from 293.15 to 308.15 K, αLA forms complexes with kaempferol, curcumin, and trans-resveratrol, with a binding constant (K_b) in the order of $10^6 M^{-1}$. In addition, they reported that this protein can act as an appropriate carrier for these bioactive compounds (MOHAMMADI; MOEENI, 2015b, 2015a).

In this context, this work aims to investigate the kinetics and thermodynamics of the formation of αLA–NR and αLA–NG complexes using the SPR technique at physiological pH and different temperatures, as well as the correlation of the SPR results with the best-binding model obtained by molecular docking.

2. Materials and methods

2.1 Materials

Bovine milk αLA (≥85 wt.%), NG (≥98 wt.%), NR (≥95 wt.%), and dimethylsulfoxide (DMSO, ≥99.9 wt.%) were purchased from Sigma-Aldrich (USA). Sodium phosphate and sodium azide (analytical grade) were acquired from Vetec (Brazil). CM5 sensor chips and coupling reagents (N-ethyl-N'-(3-dimethylaminopropyl) carbodiimide (EDC), N-hydroxysuccinimide (NHS), and ethanolamine hydrochloride) were purchased from GE Healthcare (USA). All the chemicals and reagents used were of analytical grade.

2.2 SPR analysis

SPR analysis was performed using a Biacore X100 instrument (GE Healthcare, Pittsburgh, PA, USA). In the experiment, CM5 sensor chips composed of covalently carboxymethylated dextran bonded to a gold film were used. The samples were drained on the surface of the sensor chip in two flow channels: a sample channel (immobilized αLA) and a reference channel (non-immobilized αLA). The equipment detector relates the time to the output signal, i.e., the difference in signals between the channels of the sensor chip. Thereafter, graphs called sensorgrams were generated and expressed in arbitrary resonance units (RU) in relation to time (t), where one RU corresponds to a displacement of 0.0001° in the SPR angle.

2.2.1 Preparation of the CM5 sensor chip

The CM5 sensor chip was prepared using an amine-coupling kit, according to the protocol of the manufacturer. The carboxylic groups on the sensor chip were initially activated with a 1:1 solution of EDC:NHS at a flow rate of 20 $\mu L/min$ at 298 K. The solution flowed over the surface of the CM5 for 7 min to facilitate the reaction between the carboxymethyl-dextran in CM5 and EDC–NHS.

2.2.2 Immobilization of αLA

A solution of 30 μg mL−1 of αLA flowed over the sample channel of the CM5 chip at pH 4.0 and a flow rate of 20 $\mu L/min$, forming covalent bonds between the

carboxyl groups of carboxymethyl-dextran and the αLA amino groups. Afterward, 0.1 M ethanolamine–HCl (pH: 8.5) flowed over the CM5 chip for 7 min to deactivate the excess hydroxysuccinimidyl groups on the surface that did not react with the protein. To correct the systematic noise and deviation of the instrument, a procedure similar to that described above was performed, but without the immobilization of αLA, using it as the reference surface.

2.2.3 NR and NG interactions with the immobilized αLA

The interactions of αLA with NR and NG were analyzed in triplicate at temperatures ranging from 285 K to 301 K. Solutions of NR and NG with different concentrations (20, 30, 40, 50, 60, and 70 μM; pH: 7.4; 2% v/v, DMSO) were injected into the two channels of the sensor chip (sample and reference) for 20 s at a flow rate of 10 $\mu L/min$, after which the signal (unit response; RU) was read. The selected flow rate prevents the diffusion of the analyte on the chip surface; that is, it makes it impossible for the diffusion rate to be lower than the association rate, thus avoiding the mass-transport effect. At the beginning of each binding cycle, an aliquot of the HBS-P buffer (0.01 M HEPES, 0.15 M NaCl; 0.005% v/v, P20 surfactant) was injected two times for 30 s at a flow rate of 30 $\mu L/min$ to regenerate the surface of the CM5 sensor chip.

2.3 Molecular docking

First, the structure of the αLA protein obtained by X-ray crystallography with a resolution of 2.20 Å (PDB ID: 1F6S) (CHRYSINA; BREW; ACHARYA, 2000) was retrieved from the Protein Data Bank (ANDREAEOPSIDA, 2013). The three-dimensional structures of NR (ID: ZINC8143604) and NG (ID: ZINC156701) were obtained from the ZINC15 database (STERLING; IRWIN, 2015). The ligands and proteins were prepared using the Autodock 4 program. The docking grid was adjusted using the AutoDock grid program containing all the proteins inside the analysis box. The top 10 binding modes between the ligand and protein were obtained using the AutoDock Vina program. The docking results were analyzed using PyMOL version 2.5. The electrostatic surface potential of the protein was predicted and colored using the

electrostatic surface of the functional site (eF-site) approach (KINOSHITA; NAKAMURA, 2004).

3. Results and discussion

3.1 Determination of the ligand density: αLA immobilization on the CM5 chip surface

The CM5 sensor chip has dual-flow channels on its surface: sample and reference channels (Fig. S2 in Supporting Information). To immobilize the αLA molecules in the sample channel, a mixture of EDC and NHS was used to functionalize the carboxylic groups of the carboxymethyl dextran layer. As the αLA isoelectric point was approximately at pH 4.5, acetate buffer (pH 4.0) was used to positively charge the protein surface to avoid electrostatic repulsion with the negatively charged dextran. Thus, the immobilization occurred through covalent bonds between the αLA amine groups and the dextran carboxylic groups.

We utilized a low immobilization density (4009 RU) to avoid possible mass-transport effects that would affect the determination accuracy of the interaction kinetics. The reference channel ensured that non-specific interactions were not considered in the protein–analyte interaction data. This method, known as amine coupling, is recommended by the manufacturer of the SPR device, and similar protocols have been used successfully in other protein–analyte interaction studies (LUO et al., 2020; YEKTA et al., 2020). After the appropriate modification of the chip surface with the αLA protein, the analytes, i.e., NR and NG, were introduced on the sensor surface through injections in the flow system in a controlled manner to proceed with the binding experiment.

3.2. Real-time detection of the kinetics of binding of NR or NG to immobilized αLA

The real-time detection of the association and dissociation kinetic rate constants (k_{on} and k_{off}, respectively) associated with the flavonoids–αLA complex formation is dependent on the data extracted from sensorgrams (Fig. 1). The resonant signal (RU)

vs. time curve of the immobilized αLA interacting with the flavonoids was recorded in real-time for each injection of NR and NG in different concentrations, at 298.15 K (Fig. 1a and 1b, respectively). The sensorgrams of the other temperatures studied are shown in Fig. S3 and S4 in Supporting Information for NR and NG, respectively.

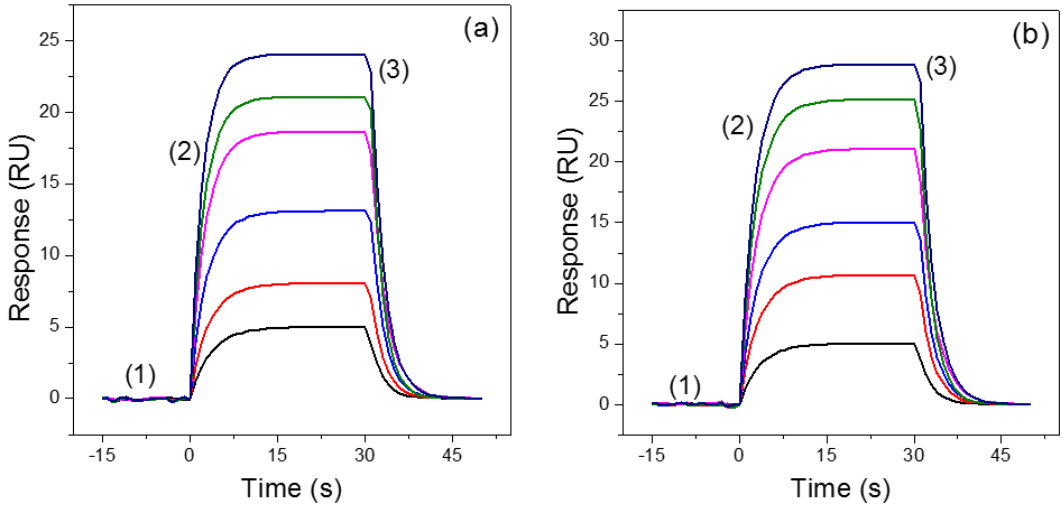

Fig. 1. SPR sensorgrams of the flavonoid interactions with the immobilized αLA on the chip surface at 298.15 K: (a) αLA-NR, and (b) αLA-NG. The aqueous solutions pumped over the chip surface are (1) HBS-P buffer (pH 7.4), (2) flavonoid suspensions (pH 7.4), and (3) HBS-P buffer (pH 7.4). The concentrations of the flavonoid suspensions were 20, 30, 40, 50, 60, and 70 μM.

To obtain the rate constants, we first constructed a baseline (region 1) by flowing only the buffer over the sample and reference chip channels. The observed rate (k_{obs}) and k_{off} constants were calculated using the global fitting of Eq. 1 and 2 (pseudo-first-order kinetic and 1:1 binding models) to the sensorgram data.

$$RU(t) = RU_{max}(t_\infty)[1 - e^{-k_{obs}(t)}], \quad \text{Eq. 1}$$

$$RU(t) = RU(t_m)\, e^{-k_{off}(t-t_m)}, \quad \text{Eq. 2}$$

where $RU(t)$ is the resonant signal obtained in the sensorgram at time t, $RU_{\max}(t_\infty)$ is the resonant signal upon protein saturation by the flavonoid, $RU(t_m)$ is the resonant signal obtained in the sensorgram at time t_m, and t_m is the time at which the dissociation process becomes predominant due to the washing off of all flavonoids on the chip surface with the buffer (beginning of region (3)).

As it was experimentally observed that $k_{obs} = k_{on} \cdot [flav] + k_{off}$, where $[flav]$ is the flavonoid concentration (Fig. S5 in Supporting Information), k_{on} was calculated using the angular coefficient of k_{obs} vs. $[flav]$ linear relationship. After the αLA-flavonoids interaction process achieved a metastable equilibrium (at 30 s), where the association and dissociation velocities are equal, only the buffer flowed through the chip channels again, decreasing the RU signal (region 3) of the sensorgram exponentially (Fig. 1).

The k_{on} values were in the range between 3.16 × 10^3 and 4.20 × 10^3 M^{-1} s^{-1} and between 1.43 × 10^3 and 2.09 × 10^3 M^{-1} s^{-1} for αLA-NR and αLA-NG interaction processes, respectively. Regarding k_{off}, the values varied from 0.41 to 0.48 s^{-1} and from 0.37 to 0.43 s^{-1} for the αLA-NR0 and αLA-NG^0 dissociation steps, respectively. The temperature influenced the k_{on} and k_{off} values of the αLA-NR0 and αLA-NG0 complex formation processes, as shown in Fig. 2.

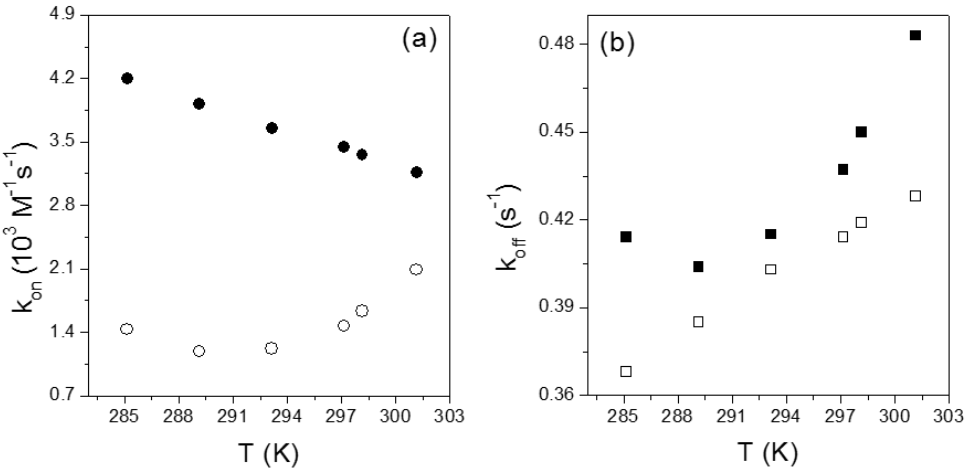

Fig. 2. Rate constants for the (a) association (k_{on}) and (b) dissociation (k_{off}) of αLA-NR0 (closed symbol, ● and ■) and αLA-NG0 (open symbol, ○ and □) as a function of temperature.

The increase in the temperature retarded the association between αLA and NR ($k_{on(\,\alpha LA-NR^0\,)} = (-6.4\mathrm{E}-2)T + 22.4$ (R2 = 0.997)) and increased the dissociation rate of the αLA-NG0 complexes ($k_{off(\,\alpha LA-NG^0)} = (3.7\mathrm{E}-3)T - 0.7$ (R2 = 0.991)). Conversely, the speed of the association of αLA with NG decreased up a temperature of 292.36 K and increased above this temperature ($k_{on(\,\alpha LA-NG^0)} = (8.7\mathrm{E}-3)T^2 - 5.0T + 732.4$ (R2 = 0.994)). The αLA-NR0 dissociation process also showed a

temperature of 289.20 K, from which it increased ($k_{off(\alpha LA-NR^0)} = (5.5\mathrm{E}-4)T^2 - 0.3T + 46.1$ (R2 = 0.996)). These results showed that the temperature effect depended on the presence of a carbohydrate group on the flavonoid molecule. The presence of the 7-neohesperidose group in NR also influenced the partition coefficients in the water–octanol system (SOUZA et al., 2020), its antioxidant (GERÇEK et al., 2021) and anti-inflammatory (AMARO et al., 2009) activities, and its adsorption to a lipid monolayer composed of DPPC (1,2-dipalmitoyl-sn-glycero-3-phosphocholine) (SOUZA et al., 2020).

The k_{on} values between αLA and NR were approximately 3.3–1.5-fold higher than that between αLA and NG, i.e., the number of αLA-NG0 complexes formed per second is higher than that of αLA-NG0 complexes at all temperatures evaluated. Furthermore, the amount of αLA-NR0 dissociated complexes formed per second was greater than that of the αLA-NG0 complexes ($k_{off(\alpha LA-NR^0)} > k_{off(\alpha LA-NG^0)}$). This demonstrates that despite NR being bulkier because of the presence of a glycoside moiety, it associates and dissociates from αLA faster than NG. This carbohydrate effect suggests that the αLA-NR0 interaction occurs via 7-neohesperidose group–amino acid residue hydrogen bonding at the protein surface, while the αLA-NG0 binding originates from the insertion of NG molecules inside the hydrophobic αLA site, which takes more time.

There is no report on protein–NG binding kinetics; further, only three studies on the kinetics of protein interaction with NR have been reported, which makes it difficult to conduct a complete comparison between our results and those from the literature. Nunes et al. (2019) and Pacheco et al. (2020) evaluated the binding kinetics between NR and LF and β-Cas proteins, respectively, by SPR under the same temperature and pH conditions used here. The k_{on} values for LF-NR and β-Cas-NR were 0.55–3.56 x 10^4 M^{-1} s^{-1} and 1.93–2.70 x 10^3 M^{-1} s^{-1}, respectively. The NR associated with LF was approximately 10-fold faster and with β-Cas 1.5-fold slower than those with αLA. Furthermore, the magnitude of the k_{off} values for LF-NR was similar to those obtained for β-Cas-NR, and both were slightly smaller (1.5 fold) than those observed for αLA-NR0. Therefore, our results were of the same order as those previously obtained. Conversely, Liu et al. (2017) obtained a k_{on} value of 7.05 M^{-1} s^{-1} and k_{off} value of 0.016 s^{-1} for the interaction between NR and α-amylase, at pH 6.0 and 298.15

K by SPR, i.e., the association and dissociation rates were 470 and 28 times lower than those for αLA, respectively.

The derivative of the function that establishes the relationship, lnk_x $(x = a, d)$ vs. $1/T$, shown in the Arrhenius plot (Fig. S6 in Supporting Information) determines the activation energy of the transition complex formation involved in the association of free interacting molecules and the dissociation of thermodynamically stable complexes. The linear dependence of lnk_x on the reciprocal temperature for the association of NR with αLA and for the dissociation of for αLA-NG0indicates that these molecular events occurred in a single step. Conversely, the dissociation of the for αLA-NR0 complex and the association between NG and αLA presented a non-linear Arrhenius plot, suggesting that these processes occurred through multiple stages (DE PAULA et al., 2020).

Considering that the 7-neohesperidose group influenced the kinetics of the association and dissociation of the flavonoids to αLA, a thermodynamic study is essential for elucidating the glycoside effect on the formation driving power of the αLA-flavonoids complexes. As previously discussed, the effect of the glycoside group may be associated with the relative contributions of hydrophobic and hydrophilic interactions to the formation of αLA-flavonoids complexes. This hydrophobic/hydrophilic balance contribution also appears in the thermodynamic parameters of the complex formation.

3.3. Effect of the flavonoid hydrophobicity/hydrophilicity balance on the thermodynamics of interaction with αLA

The binding constant (K_b, M^{-1}) was determined from the relationship between the kinetic rate constants ($K_b = k_{on}/k_{off}$). The standard Gibbs free energy change (ΔG^0, kJ mol^{-1}) of the $\alpha LA - \text{flav}$ complex formation was obtained from the following equation: $\Delta G^0 = -RTlnK_b$ (where T is the temperature in K, and R is the universal gas constant (8.3145 J mol^{-1} K^{-1})). The standard enthalpy change (ΔH^0, kJ mol^{-1}) was found to fit lnK_b vs. $^1/_T$ data to a non-linear van't Hoff model (Eq. 3), followed by its derivation, resulting in Eq. 4 (Fig. S7 in Supporting Information) (de Paula et al., 2020; Lelis et al., 2017; Nunes et al., 2017; Rezende et al., 2017).

$$lnK_b = a + b\left(\frac{1}{T}\right) + c\left(\frac{1}{T}\right)^2 + d\left(\frac{1}{T}\right)^3, \quad \text{Eq. 3}$$

$$\Delta H^0 = -R\left[b + 2c\left(\frac{1}{T}\right) + 3d\left(\frac{1}{T}\right)^2\right], \quad \text{Eq. 4}$$

where a, b, c, and d are constants that can be graphically determined using polynomial adjustment.

Finally, the well-known Gibbs fundamental relationship, i.e., $\Delta G^o = \Delta H^0 - \mathrm{T}\Delta S^0$, provided the entropic term ($T\Delta S^0$, kJ mol^{-1}) for the complex-formation process. Table 1 lists all the thermodynamic parameters obtained for the αLA-flavonoids interactions.

Table 1. Thermodynamic parameters: binding constant (K_b) and standard changes in the Gibbs free energy (ΔG^0), enthalpy (ΔH^0), and entropy ($T\Delta S^0$) for the formation of the $\alpha LA - NR^0$ and $\alpha LA - NG^0$ complexes at different temperatures (T) and pH 7.4.

* For all the parameters, the standard deviation did not exceed 4%.

T	$\alpha LA - NR^0$				$\alpha LA - NG^0$			
	K_b	ΔH^0	ΔG^0	$T\Delta S^0$	K_b	ΔH^0	ΔG^0	$T\Delta S^0$
K	10^3 M^{-1}	kJ mol^{-1}			10^3 M^{-1}	kJ mol^{-1}		
285.15	10.15	-6.43	-21.87	15.44	3.88	-60.00	-19.59	-40.41
289.15	9.70	-11.67	-22.07	10.40	3.09	-20.12	-19.32	-0.80
293.15	8.79	-18.77	-22.13	3.36	3.03	14.64	-19.54	34.18
297.15	7.88	-27.57	-22.17	-5.41	3.55	44.66	-20.19	64.85
298.15	7.47	-30.02	-22.11	-7.91	3.89	51.46	-20.49	71.95
301.15	6.54	-37.93	-22.00	-15.94	4.88	70.27	-21.26	91.53

The K_b values for the $\alpha LA - NR^0$ complex were almost two times those for the $\alpha LA - NG^0$ complex. For the temperature range studied, as the temperature increased, the number of $\alpha LA - NR^0$ complexes decreased monotonically. In contrast, with an increase in temperature until 291.70 K, the K_b values decreased, whereas above this temperature, the formation amount of the $\alpha LA - NG^0$ complexes increased ($K_{b(\alpha LA - NG^0)} = 21.450T^2 - 1.251\mathrm{E}4T + 1.828\mathrm{E}6$ (R2 = 0.996) (Fig. S8a in Supporting Information).

Das et al. (2018) obtained the K_b constant for the complexes between NR and NG with lysozyme (LYS) using the fluorescence spectroscopy (FS) technique at 300 K

and pH 7.4. Despite the structural chemical similarity between the LYS and αLA proteins, to the point where they are considered homologous (BREW, 2011), the K_b values for the complexes formed with LYS (10^4 M^{-1}) were approximately 10-fold greater than those for the complexes formed with αLA (10^3 M^{-1}). In addition, for the Lysozyme-flavonoids interaction, the K_b magnitude order was contrary to our results, i.e., $K_b(LYS-NG) > K_b(LYS-NR)$. The FS technique is sensitive only to interaction events that occur at protein sites that have fluorescent amino acid residues; conversely, SPR detects interactions in all kinds of protein sites. Thus, in other studies comparing the K_b constants obtained by FS and SPR for complexes between proteins and small molecules, the following result was also obtained, $K_{b-SPR} < K_{b-FS}$, owing to the presence of other non-fluorescent interaction sites that participate in the interaction and interfere with the obtained K_b value from the SPR binding experiment (Bahri et al., 2019; Hudson et al., 2018; Lelis et al., 2017; Rezende et al., 2020a).

The K_b values for the LF-NR complex obtained by SPR and in the same temperature range used in our study were in the order of 10^4 and 10^5 M^{-1}, increasing polynomially with the temperature, passing through a maximum K_b at 295.62 K (Nunes et al., 2019). For the β-Cas-NR complex, the K_b values were of the order of 10^3 M^{-1}, increasing linearly with the temperature. These different effects of temperature on the K_b behavior demonstrate that NR interacts with distinct proteins in sites containing different amino acid residues.

The effect of the chemical structure of flavonoids, as well as the influence of temperature on the K_b values may originate from two sources: configurational changes (positive $T\Delta S^0$) or specific intermolecular interactions (negative ΔH^0).

The ΔH^0 values (Table 1) for the formation of αLA-NR0 were negative for all temperatures investigated, while the $T\Delta S^0$ values (Table 1) were positive until 293.98 K, and above this temperature, negative values were obtained. The deprotonation steps of the ionizable OH groups of NR occur in the pH range of 8–12 (MIELCZAREK, 2005); therefore, the pH at which the interaction study was carried out (7.4), NR was predominantly in its neutral form, and electrostatic interactions were not the main contributors to the αLA-NR0 interaction. The ΔH^0 and $T\Delta S^0$ values together with the six OH groups present in the NR glycoside (Fig. S1) highlight that hydrogen bonding prevailed during the formation of the αLA-NR0 complex.

The higher the temperature, the lower the ΔH^0 and $T\Delta S^0$ values (Table 1). Considering that H bonds are cooperative and orientated interactions, the OH groups of the interacting molecules should have some degree of rotational freedom to be orientated in the space to form H bonds (RASCHKA et al., 2018). At relatively low temperatures, the system had a low molecular average kinetic energy ($^3/_2 KT$), preventing the glycoside groups of NR from overcoming the energetic rotational barrier through energy transfer by molecular collisions. Therefore, there is a small yield of H bonds, and few bonds were formed between NR and the carboxylic groups of the αLA amino acid residues. This can explain the negative but small (in modulus) ΔH^0 values at low temperatures. Similarly, we can assume the positive $T\Delta S^0$ values (up to 293.98 K), owing to the configurational entropy (resulting from the solvation of αLA and NR molecules), overcame the rotational entropy (since only a few H bonds were formed at low temperatures).

As the temperature increased, the kinetic energy of the glycoside NR groups allowed the rotation of OH groups required for H bonding; thus, the H bonds were optimized, releasing a considerable amount of energy, which in turn resulted in a more negative ΔH^0 value. As a result of the orientation and cooperativity provided by the formation of many H bonds, the rotational entropy predominated over the configurational entropy, reducing the entropic term.

In contrast, the ΔH^0 and $T\Delta S^0$ values for the formation of the αLA-NG0 complex showed opposite behavior compared to those observed for αLA-NR0. This could be explained by the higher NG hydrophobicity compared to that of NR, enabling the interaction of the former in the protein core. At temperatures below 291.36 K, both ΔH^0 and $T\Delta S^0$ were negative because the molecular kinetic average energy was relatively small; therefore, the energy transferred from molecular collisions was not enough to overcome the potential energy barrier associated with the conformational changes of the αLA site. This means that at relatively low temperatures, the αLA binding site is less flexible, preventing NG from penetrating more internal sites of the protein. In this case, a small number of water molecules is released from the solvation layer of the reagents; that is, the cost of desolvation and entropic gain was also low. As the temperature increased, the molecular average kinetic energy increased, which consequently enhanced the energy transferred through molecular collisions. Consequently, the penetration degree of NG inside the αLA sites increased, inducing

conformational changes and the desolvation of interacting molecules. Therefore, ΔH^0 and $T\Delta S^0$ are positive (de Paula et al., 2020; Nunes et al., 2019; Rezende et al., 2020).

The low-temperature influence on the ΔG^0 values despite its remarkable effect on ΔH^0 and $T\Delta S^0$ indicated enthalpic–entropic compensation (EEC; Fig. S9 in Supporting Information), a phenomenon that occurs in both systems. The EEC implies that as the temperature increases, there is a concomitant decrease in the ΔH^0 values with a proportional decrease in the entropic term, resulting in the efficient optimization of the energetic cost to form the αLA-flavonoids complexes.

The rate of change of ΔH^0 with temperature ($\partial \Delta H^0 / \partial T$), under constant pressure, provides the parameter of the standard heat capacity change (ΔC_p^0) (Fig. S10 in Supporting Information). The ΔC_p^0 for the αLA-NG0 complex formation was positive ($\Delta C_{p\ \alpha LA-NG^0}^0$ = 8.15 kJ.mol^{-1}.K^{-1}, R2 = 0.992), while the that for αLA-NR0 was negative ($\Delta C_{p\ \alpha LA-NR^0}^0$ = -1.96 kJ.mol^{-1}.K^{-1}, R2 = 0.982). Considering that the temperature and pressure conditions, as well as the number of molecules and the pH of the medium were the same for both systems, the $\Delta C_{p\ \alpha LA-NG^0}^0 > \Delta C_{p\ \alpha LA-NR^0}^0$ relationship shows that when receiving energy in the form of heat, the αLA-NG0 system has a higher capacity to store this energy in the potential form than the αLA-NR0 system. This indicates that the number and intensity of intermolecular interactions involved in the formation of the αLA-NG0 complex are higher than those for αLA-NR0. These interactions could be associated with specific αLA-flavonoids or even αLA-water, flavonoids-water, or water-water interactions.

3.4. Effect of flavonoid hydrophobicity on the formation of intermediate structures

From the analysis of the Arrhenius plot (Fig. S5 in Supporting Information), it is possible to obtain energetic parameters related to the formation of thermodynamically unstable complexes known as transition (or activated) complexes. These complexes are chemical entities that occur in the path of interaction between thermodynamically stable chemical structures, i.e., between free reagents and the complexes formed. The instability of these complexes is attributed to their very high energetic content; therefore, their existence occurs in such short time spaces, which prevents their

experimental observation. Evans and Polanyi (1935) defined the transition state as “an infinitesimally thin layer of phase space.” Thus, the formation of the transition complex occurs by both the association of free molecules and the dissociation of the stable thermodynamic complex ($\alpha LA + \mathrm{flav} \rightleftarrows (\alpha\mathrm{LA} - \mathrm{flav}^{\ddagger}) \leftrightarrows (\alpha\mathrm{LA} - \mathrm{flav}^{0})$ (ARANGO-RESTREPO; RUBI; BARRAGÁN, 2018; REZENDE et al., 2020b).

The dependence relationship of lnk_{on} and lnk_{off} with the temperature expressed in Eq. 5 provides the activation energy ($E_{act\,(y)}$, kJ mol−1) for the formation of a transition complex ($\alpha\mathrm{LA} - \mathrm{flav}^{\ddagger}$) from the association of the protein with the flavonoids ($y = on$) or from the dissociation of the formed $\alpha LA - \mathrm{flav}^{0}$ complex ($y = off$).

$$E_{act\,(y)} = -R\left(\frac{dlnk_y}{dT}\right), \qquad \text{Eq. 5}$$

where k_y is the rate constant at temperature T (K) and R is the universal gas constant (8.314 J mol−1 K−1).

The other energetic parameters were calculated from the mathematical relationships expressed in Eq. 6 – 8 (WANG; ROBERTS, 2013):

$$k_y = \frac{k_B T}{h}\exp\left(\frac{-\Delta G_y^{\ddagger}}{RT}\right), \qquad \text{Eq. 6}$$

$$\Delta H_y^{\ddagger}(T) = E_{act(y)}(T) - RT, \qquad \text{Eq. 7}$$

$$T\Delta S_y^{\ddagger}(T) = \Delta H_y^{\ddagger}(T) - \Delta G_y^{\ddagger}(T), \qquad \text{Eq. 8}$$

where $\Delta G_y^{\ddagger}$ is the activation Gibbs free energy change (kJ mol−1), $\Delta H_y^{\ddagger}$ is the activation enthalpy change (kJ mol−1), and $T\Delta S_y^{\ddagger}$ is the activation entropy change (kJ mol−1). k_B is the Boltzmann constant (1.38066 × 10^{-23} J K^{-1}) and h is Planck’s constant (6.62608 × 10^{-34} J s) at temperature T (K).

3.4.1. Transition-complex formation from the association: $\boldsymbol{\alpha\mathrm{LA} + \mathrm{flav} \rightleftarrows \alpha\mathrm{LA} - \mathrm{flav}^{\ddagger}}$

Fig. 3 shows the behavior of the energy parameters for the formation of the $\alpha\mathrm{LA} - \mathrm{flav}^{\ddagger}$ complex with temperature variation.

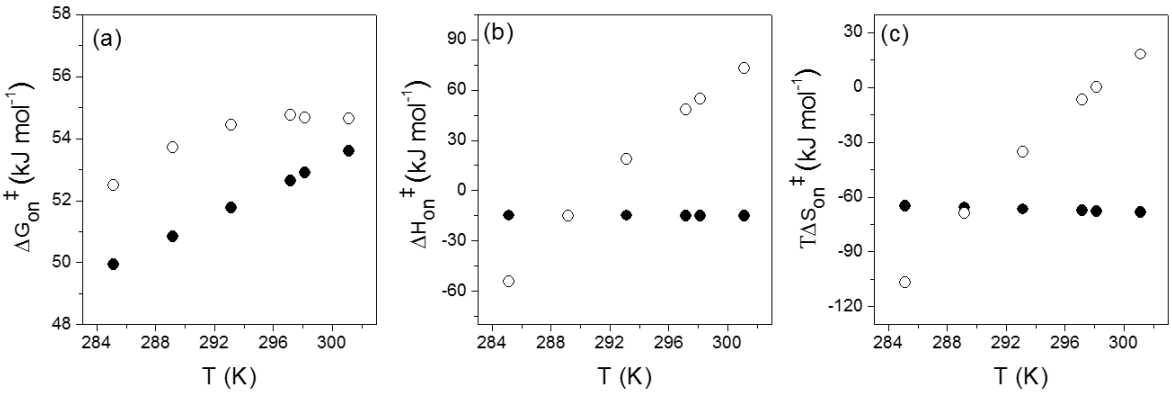

Fig. 3. Energetic parameters for the formation of the transition complex from the association of NR (●) or NG (○) with αLA as a function of temperature, at pH 7.4. (a) Activation Gibbs free energy change ($\Delta G_{on}^{\ddagger}$), (b) activation enthalpy change ($\Delta H_{on}^{\ddagger}$), and (c) activation entropy change ($T\Delta S_{on}^{\ddagger}$).

The rate of formation of the transition complex with αLA was higher for NR than for NG (Fig. 3a).

The negative values of $E_{act\ on;\ \alpha LA-NR^{\ddagger}}$ (-12.43 kJ mol−1), the enthalpic and entropic energies, and their respective small variations as a function of temperature ($\alpha_{\Delta H_{on}^{\ddagger}\ vs\ T;\ \alpha LA-NR^{\ddagger}} = -0.008$ kJ mol^{-1} K^{-1} (Fig. 3b, R2 = 0.996) and $\alpha_{T\Delta S_{on}^{\ddagger}\ vs\ T;\ \alpha LA-NR^{\ddagger}} = -0.235$ kJ mol^{-1} K^{-1} (Fig. 3c, R2 = 0.999)) showed that hydrophilic interactions (H bonds) were predominant for the formation of the $\alpha LA - NR^{\ddagger}$ complex occurring on the protein surface. Therefore, low desolvation of interacting molecules and conformational changes were observed, which were slightly influenced by the temperature. Interestingly, the $E_{act(on)}$ for the transition complex formed by NR interacting with a highly hydrophobic protein (β-Cas) showed a positive value (15.07 kJ mol−1) (PACHECO et al., 2020), which indicated that the driving force for the transition complex formation was dependent on the hydrophobicity/hydrophilicity of the protein sites.

Conversely, the values of $E_{act(on);\ \alpha LA-NG^{\ddagger}}$ were temperature-dependent and varied from -51.80 to 75.35 kJ mol−1 between 285.15 and 301.15 K. The association

between NG and αLA to form the transition complex was enthalpically driven up to 291.36 K and entropically favorable above 298.26 K ($\Delta H^{\ddagger}_{on\,;\,\alpha LA-NG^{\ddagger}} = 7.950T - 2316.331$ (Fig. 3b, R2 = 0.991) and $T\Delta S^{\ddagger}_{on\,;\,\alpha LA-NG^{\ddagger}} = 7.817T - 2331.484$ (Fig. 3c, R2 = 0.992)). Therefore, for the $\alpha LA - NG^{\ddagger}$ complex formation, the interaction was mostly hydrophobic, i.e., the difference in the 3D structure of water from the solvation shell of the hydrophobic region of the protein and from the bulk determined the energetic costs for the complex formation. The higher the temperature, the higher the structural difference, similar to the case for the thermodynamic behavior.

3.4.2. Transition-complex formation from the dissociation: $\boldsymbol{\alpha LA - flav^{0} \rightleftarrows \alpha LA - flav^{\ddagger}}$

The effect of temperature on the changes in the energetic parameters for the formation process of the $\alpha LA - flav^{\ddagger}$ transition complex from the dissociation of the $\alpha LA - flav^{0}$ stable thermodynamic complex is graphically shown in Fig. 4.

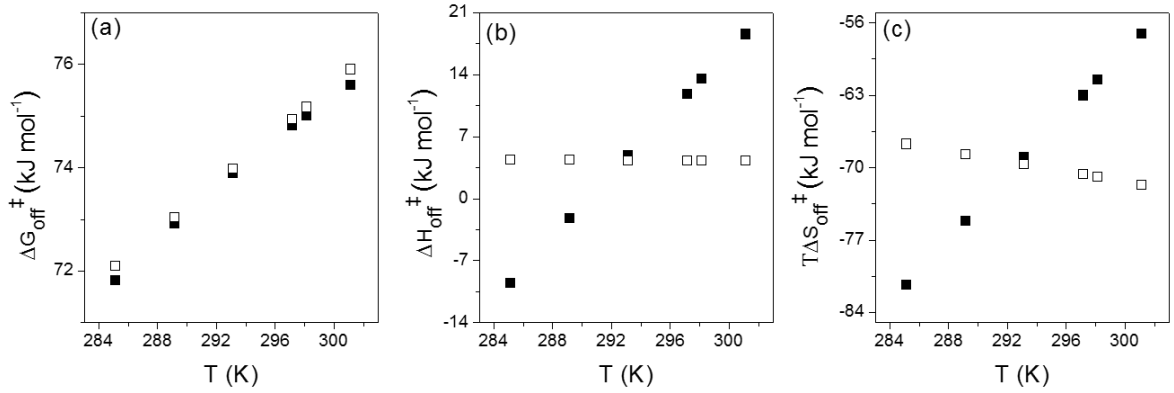

Fig. 4. Energetic parameters for the formation of the transition complex from the dissociation of $\alpha LA - NR^{0}$(■) or $\alpha LA - NG^{0}$(□) as a function of temperature, at pH 7.4. (a) Activation Gibbs free energy change ($\Delta G^{\ddagger}_{off}$), (b) activation enthalpy change ($\Delta H^{\ddagger}_{off}$), and (c) activation entropy change ($T\Delta S^{\ddagger}_{off}$).

The rates of formation of transition complexes from the dissociation of the stable complexes were independent of the flavonoids involved in the interaction with the protein ($\Delta G^{\ddagger}_{off;\,\alpha LA-NR^{\ddagger}} \cong (\Delta G^{\ddagger}_{off;\,\alpha LA-NG^{\ddagger}}$, Fig. 4a). However, the energy required to

dissociate the stable complexes differed among the studied flavonoids. For the formation of $\alpha LA - NR^{\ddagger}$, $E_{act(off)}$ was dependent on temperature and varied from -7.19 to 21.06 kJ mol^{-1}, while for $\alpha LA - NG^{\ddagger}$, the energy was 6.74 kJ mol^{-1} for all the evaluated temperatures.

The positive values of $\Delta H^{\ddagger}_{off}$ and negative values of $T\Delta S^{\ddagger}_{off}$ for the formation of $\alpha LA - NG^{\ddagger}$ varied slightly as the temperature increased ($\Delta H^{\ddagger}_{off;\, \alpha LA-NG^{\ddagger}} \approx 4.3$ kJ mol^{-1} ($\alpha_{\Delta H^{\ddagger}_{off}\, vs\, T;\, \alpha LA-NG^{\ddagger}} = -0.008$ kJ mol^{-1} K^{-1} (Fig. 4b, R2 = 0.995), and $T\Delta S^{\ddagger}_{off;\, \alpha LA-NG^{\ddagger}} \approx -70.0$ kJ mol-1 ($\alpha_{T\Delta S^{\ddagger}_{off}\, vs\, T;\, \alpha LA-NG^{\ddagger}} = -0.246$ kJ mol^{-1} K^{-1} (Fig. 4c, R2 = 0.999)). This behavior indicated that the formation of the thermodynamically stable complex from the $\alpha LA - NG^{\ddagger}$ complex was dependent on the desolvation of the energetically unfavorable structure, which increased the total entropy of the system. Therefore, the molecular process of binding-site fitting required for the formation of $\alpha LA - NG^{0}$ occurred with high intensity during the association of the free molecules, which preceded the formation of the transition complex.

Contrarily, the enthalpic and entropic energies necessary for the formation of $\alpha LA - NR^{\ddagger}$ were temperature-dependent. At temperatures up to 290.44 K, the $\alpha LA - NR^{\ddagger}$ formation process was enthalpically favorable ($\Delta H^{\ddagger}_{off;\, \alpha LA-NR^{\ddagger}} = 1.758T - 510.596$ (Fig. 4b, R2 = 0.999)). Above 290.44 K, the formation of the transition complex began to incur both enthalpic and entropic costs. These findings demonstrate that conformational changes to the protein binding-site fitting occur during the dissociation of the thermodynamically stable complex.

3.5 Molecular-docking analysis

To evaluate the potential molecular mechanism during the NG or NR and αLA interaction, molecular docking was carried out. Both molecules were predicted to interact at the same site on the protein (Fig. 5). The binding site was composed of hydrophobic amino acids (valine, isoleucine, leucine, and tyrosine), uncharged polar amino acids (glutamine and threonine), and acidic amino acids (aspartate) (Fig. 5a). Although the absolute value of the free energy predicted by docking in both models was greater than that calculated by SPR, the interaction of the protein with NG was more stable than that with NR, which was consistent with the experimental results (Fig.

5b and 5d). Flavonoids were predicted to primarily interact with hydrophobic amino acids through non-polar interactions. (Fig. 5c and 5e). In contrast, the glycoside portion of NR showed complementary interactions with polar amino acids, aiding in stabilizing the interaction. The polar interactions formed by NR glycosides were in agreement with the negative enthalpy obtained for NG, and the absence of these polar contacts with the protein and NR justified the positive enthalpy for this complex determined by SPR analysis.

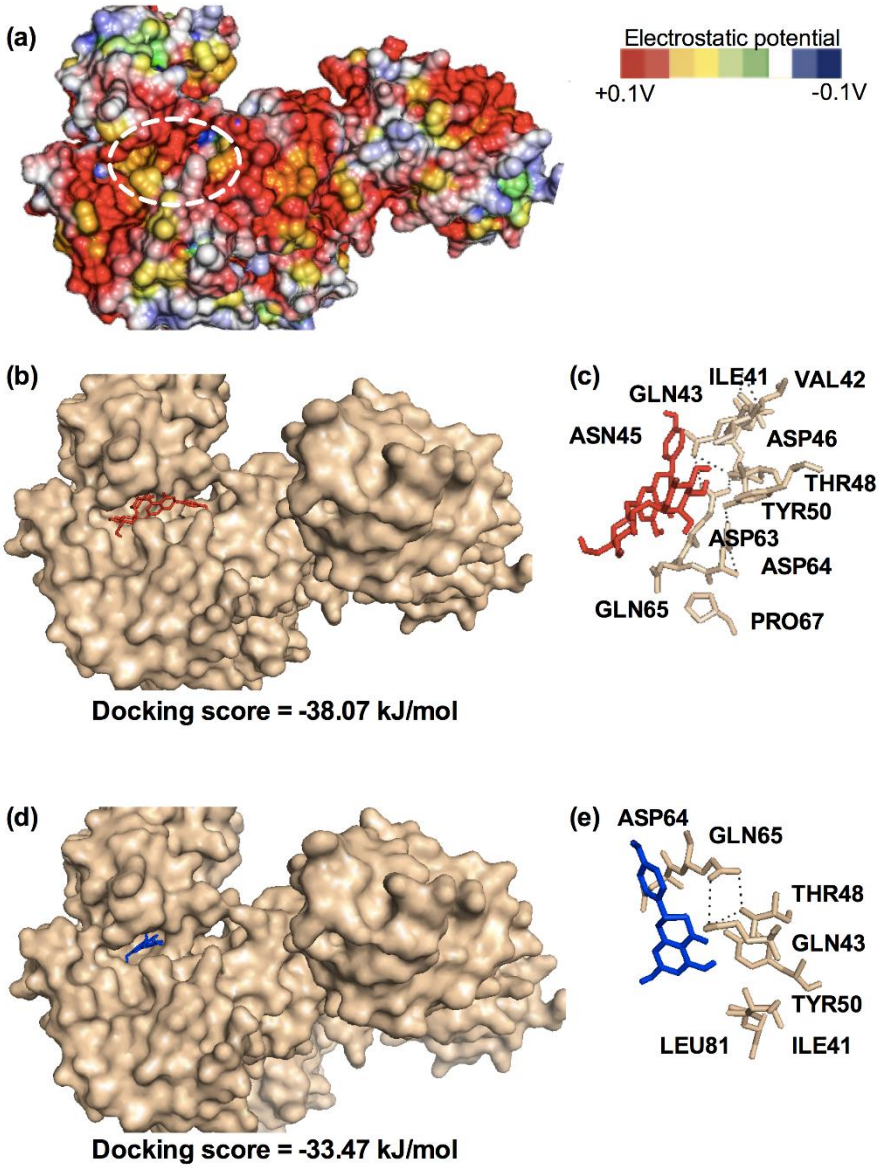

Fig. 5. Molecular-docking modeling of the αLA-NG and αLA-NR complex. a) Electrostatic potential of the protein surface. b) The best docking model of the $\alpha\mathrm{LA\ (beige\ surface)} - NG\ (\mathrm{red\ lines})$ complex. c) Detailed amino acids that interact with NG. d) The best docking model of the $\alpha\mathrm{LA\ (beige\ surface)} - NR\ (\mathrm{red\ lines})$

complex. e) Detailed amino acids that interact with NR. The black, dashed lines indicate the predicted polar contacts between the ligand and amino acid.

4. Conclusions

The variation in the RU signal after the injection of the analytes in the SPR-binding experiment confirmed the existence of an interaction between the immobilized protein and the flavonoids that flowed over the chip surface.

Regardless of the evaluation temperature, the association and dissociation rates between αLA and NR were higher than those between αLA and NG. Furthermore, the temperature variation from 285.15 to 301.15 K increased the number of $\alpha LA - NG^0$ complexes formed per second by 45% while decreasing the number of $\alpha LA - NR^0$ complexes formed by 25%.

The hydrophobicity of the flavonoid influenced the hydrophobic–hydrophilic balance in the interaction with αLA. For NR, the hydrophilic interactions were predominant at all temperatures evaluated because of its constituent glycoside group. Further, the entropic cost for accessing the protein-binding site was quite low, which was probably closer to the protein interface compared to the interaction site for NG. Conversely, for the αLA-NG0 interaction, as the temperature increased, the αLA site became increasingly flexible, favoring the penetration of NG into more hydrophobic regions of αLA. This behavior, characterized as a hydrophobic effect, further enhanced the interaction between the molecules.

The energetic parameters for the formation of the activated complexes suggested that the binding-site fitting processes for the formation of the stable thermodynamic complex occurred with high intensity during the transition between the free molecules (αLA and NG) and $\alpha LA - NG^{\ddagger}$. In contrast, to afford the αLA-NR0 complex, the $\alpha LA - NR^{\ddagger}$ complex underwent conformational changes.

The binding models of NG and NR with αLA obtained by molecular docking agreed with the results and conclusions obtained by SPR analysis. The best binding models indicated that the αLA – NG complex was more stable than αLA-NR because it underwent a high number of interactions with protein amino acids, facilitated by the glycidic portion of the molecule. Furthermore, these interactions were primarily polar, contributing to the observed negative enthalpy.

The findings of this study may contribute to optimization, as well as pharmacokinetic and pharmacodynamic prediction studies for the application of these complexes in different areas.

Funding

This work was supported by the Coordenação de Aperfeiçoamento de Pessoal de Nível Superior (CAPES), Conselho Nacional de Desenvolvimento Científico e Tecnológico (CNPq), and Fundação de Apoio à Pesquisa de Minas Gerais (FAPEMIG).

Declaration of competing interest

The authors declare that they have no known competing financial interests or personal relationships that could have appeared to influence the work reported in this paper.

5. References

ABBAS, M. M.; YOUNIS, K. M.; HUSSAIN, W. S. **Impact of medicinal plants on corona pandemic.** Plant Cell Biotechnology and Molecular Biology, v. 22, n. 19–20, p. 62–72, 2021.

ABDELLI, I. et al. I**n silico evaluation of phenolic compounds as inhibitors of A-amylase and A-glucosidase.** Journal of Biomolecular Structure and Dynamics, v. 39, n. 3, p. 816–822, 2021.

ADEBIYI, O. A.; ADEBIYI, O. O.; OWIRA, P. M. O. **Naringin reduces hyperglycemia-induced cardiac fibrosis by relieving oxidative stress**. PLoS ONE, v. 11, n. 3, p. 1–15, 2016.

AL-DOSARI, D. I. et al. **Flavonoid naringenin attenuates oxidative stress, apoptosis and improves neurotrophic effects in the diabetic rat retina.** Nutrients, v. 9, n. 10, 2017.

AL-SHABIB, N. A. et al. **Molecular interactions of food additive dye quinoline yellow (Qy) with alpha-lactalbumin: Spectroscopic and computational studies**. Journal of Molecular Liquids, v. 311, p. 113215, 2020.

ALAM, M. A. et al. **Effect of citrus flavonoids, naringin and naringenin, on metabolic syndrome and their mechanisms of action**. Advances in Nutrition, v. 5, n. 4, p. 404–417, 2014.

AMARO, M. I. et al. **Anti-inflammatory activity of naringin and the biosynthesised naringenin by naringinase immobilized in microstructured materials in a model of DSS-induced colitis in mice.** Food Research International, v. 42, n. 8, p. 1010–1017, out. 2009.

ARANGO-RESTREPO, A.; RUBI, J. M.; BARRAGÁN, D. **Kinetics and energetics of chemical reactions through intermediate states**. Physica A: Statistical Mechanics and its Applications, v. 509, p. 86–96, nov. 2018.

AVWIOROKO, O. J. et al. **Investigation of the binding interaction of α-amylase with Chrysophyllum albidum seed extract and its silver nanoparticles: A multi-spectroscopic approach**. Chemical Data Collections, v. 29, p. 100517, 2020.

BAER-DUBOWSKA, W. et al. **Tannic Acid: Specific Form of Tannins in Cancer Chemoprevention and Therapy-Old and New Applications**. Current Pharmacology Reports, v. 6, n. 2, p. 28–37, 2020.

BAHRI, A. et al. **Binding analysis between monomeric β-casein and hydrophobic bioactive compounds investigated by surface plasmon resonance and fluorescence spectroscopy.** Food Chemistry, v. 286, n. January, p. 289–296, 2019.

BELHAOUES, S.; AMRI, S.; BENSOUILAH, M. **Major phenolic compounds, antioxidant and antibacterial activities of Anthemis praecox Link aerial parts.** South African Journal of Botany, v. 131, p. 200–205, 2020.

BHARGAVA, N. et al. A**dvances in application of ultrasound in food processing: A review.** Ultrasonics Sonochemistry, v. 70, p. 105293, 2021.

BOUDET, A. M. **Evolution and current status of research in phenolic compounds.** Phytochemistry, v. 68, n. 22–24, p. 2722–2735, 2007.

BREW, K. M**ilk Proteins | α-Lactalbumin**. In: Encyclopedia of Dairy Sciences. [s.l.] Elsevier, 2011. p. 780–786.

BUITIMEA-CANTÚA, N. E.; GUTIÉRREZ-URIBE, J. A.; SERNA-SALDÍVAR, S. O. **Phenolic-protein interactions: Effects on food properties and health benefits.** Journal of Medicinal Food, v. 21, n. 2, p. 188–198, 2018.

BUJALOWSKI, W.; JEZEWSKA, M. J. **Quantitative thermodynamic analyses of spectroscopic titration curves.** Journal of Molecular Structure, v. 1077, p. 40–50, dez. 2014.

CALLIS, P. R. **Binding phenomena and fluorescence quenching. I: Descriptive quantum principles of fluorescence quenching using a supermolecule approach**. Journal of Molecular Structure, v. 1077, p. 14–21, 2014a.

CALLIS, P. R. **Binding phenomena and fluorescence quenching. II: Photophysics of aromatic residues and dependence of fluorescence spectra on protein conformation**. **J**ournal of Molecular Structure, v. 1077, p. 22–29, dez. 2014b.

CAO, D. et al. **Expression of recombinant human lysozyme in egg whites of transgenic hens.** PLoS ONE, v. 10, n. 2, p. 1–15, 2015.

CHEN, C. et al. **Effect of interactions between glycosylated protein and tannic acid on the physicochemical stability of Pickering emulsions**. Lwt, v. 152, n. 68, p. 112383, 2021.

CHRYSINA, E. D.; BREW, K.; ACHARYA, K. R. **Crystal structures of Apo- and holo-bovine α-lactalbumin at 2.2-Å resolution reveal an effect of calcium on inter-lobe**

interactions. Journal of Biological Chemistry, v. 275, n. 47, p. 37021–37029, 2000.

COMPANY, P. **SEPARATION OF HUMAN a-AMYLASE ISOZYMES BY ELECTRO-FOCUSING AND THEIR IMMUNOLOGICAL PROPERTIES**. 1975.

COUTO, M. et al. **Alergia às proteínas do leite de vaca em adolescente com anafilaxia: uma opção terapêutica inovadora**. GE Jornal Português de Gastrenterologia, v. 19, n. 6, p. 318–322, 2012.

DAS, S. et al. **Binding of naringin and naringenin with hen egg white lysozyme: A spectroscopic investigation and molecular docking study**. **Spectrochimica Acta** - Part A: Molecular and Biomolecular Spectroscopy, v. 192, p. 211–221, 2018a.

DAS, S. et al. **Binding of naringin and naringenin with hen egg white lysozyme: A spectroscopic investigation and molecular docking study**. Spectrochimica Acta Part A: Molecular and Biomolecular Spectroscopy, v. 192, p. 211–221, mar. 2018b.

DE PAULA, H. M. C. et al. **Activated Complex Approach to Describe Bovine Serum Albumin-Azure A and Bovine Serum Albumin-Azure B Intermolecular Interactions.** Journal of the Brazilian Chemical Society, 2020.

DE WIT, J. N. **Nutritional and Functional Characteristics of Whey Proteins in Food Products**. Journal of Dairy Science, v. 81, n. 3, p. 597–608, 1998.

DELAVARI, B. et al. **Alpha-lactalbumin: A new carrier for vitamin D3 food enrichment.** Food Hydrocolloids, v. 45, p. 124–131, 2015.

DUY, C.; FITTER, J. **How aggregation and conformational scrambling of unfolded states govern fluorescence emission spectra.** Biophysical Journa**l**, v. 90, n. 10, p. 3704–3711, 2006.

ESOBI, I. C.; LASODE, M. K.; BARRIGUETE, M. O. F. **The Impact of COVID-19 on Healthy Eating Habits.** Journal of Clinical Nutrition and Health, v. 1, n. 1, p. 1–2, 2020.

EVANS, M. G.; POLANYI, M. **Some applications of the transition state method to the calculation of reaction velocities, especially in solution. T**ransactions of the Faraday Society, v. 31, n. 0, p. 875–894, 1935.

FABER, C. et al. S**tudy of the Solubility of a Modified Bacillus licheniformis r - Amylase around the Isoelectric Point**. p. 707–713, 2007.

FLEMING, A. Downloaded from https://royalsocietypublishing.org/ on 01 August 2021 On a Remarkable Bacteriolytic Element found Downloaded from https://royalsocietypublishing.org/ on 01 August 2021. 1920.

FORSYTHE, E. L. et al. **Crystallization of chicken egg white lysozyme from assorted sulfate salts**. Journal of Crystal Growth, v. 196, n. 2–4, p. 332–343, 1999.

GERÇEK, E. et al. **Biochemical changes and antioxidant capacity of naringin and naringenin against malathion toxicity in Saccharomyces cerevisiae**. Comparative Biochemistry and Physiology Part - C: Toxicology and Pharmacology, v. 241, p. 108969, mar. 2021.

GHOLAMI, S.; BORDBAR, A. K. E**xploring binding properties of naringenin with bovine β- lactoglobulin: A fluorescence, molecular docking and molecular dynamics simulation study.** Biophysical Chemistry, v. 187–188, p. 33–42, 2014.

GHOSH, K.; RATHI, S.; ARORA, D. **Fluorescence spectral studies on interaction of fluorescent probes with Bovine Serum Albumin (BSA)**. Journal of Luminescence, v. 175, p. 135–140, 2016.

HAMDANI, A. M. et al. **Effect of guar gum conjugation on functional, antioxidant and antimicrobial activity of egg white lysozyme**. Food Chemistry, v. 240, n. August 2017, p. 1201–1209, 2018.

HE, Z. et al. I**nteraction of β-casein with (−)-epigallocatechin-3-gallate assayed by fluorescence quenching: effect of thermal processing temperature.** International Journal of Food Science & Technology, v. 51, n. 2, p. 342–348, fev. 2016.

HEIDARY MOGHADDAM, R. et al. **Naringenin and naringin in cardiovascular disease prevention: A preclinical review.** European Journal of Pharmacology, v. 887, n. June, p. 173535, 2020.

HILAIRE, M. R. et al. **Blue fluorescent amino acid for biological spectroscopy and microscopy.** Proceedings of the National Academy of Sciences of the United States of America, v. 114, n. 23, p. 6005–6009, 2017.

HUDSON, E. A. et al. **Thermodynamic and kinetic analyses of curcumin and bovine serum albumin binding**. Food Chemistry, v. 242, p. 505–512, mar. 2018.

HUDSON, E. A. et al. **Curcumin-micellar casein multisite interactions elucidated by surface plasmon .** International Journal of Biological Macromo, v. 133, p. 860–866, 2019.

HUI, X. et al. **The effects of bioactive compounds from blueberry and blackcurrant powders on the inhibitory activities of oat bran pastes against α-amylase and α-glucosidase linked to type 2 diabetes**. Food Research International, v. 138, n. PA, p. 109756, 2020.

JI, Y. et al. **α -glucosidase and α -amylase**. v. 145, n. April, 2021.

KACZMAREK, B. **Tannic acid with antiviral and antibacterial activity as a promising component of biomaterials-A minireview**. Materials, v. 13, n. 14, 2020.

KAMAU, S. M. et al. **Alpha-lactalbumin: Its production technologies and bioactive peptides.** Comprehensive Reviews in Food Science and Food Safety, v. 9, n. 2, p. 197–212, 2010.

KANDRA, L. et al. **Inhibitory effects of tannin on human salivary α-amylase.** Biochemical and Biophysical Research Communications, v. 319, n. 4, p. 1265–1271, 2004.

KHAN, I. et al. **Lisozima como agente antiproliferativo para bloquear a interação entre S100A6 e o domínio RAGE** V. p. 1–9, 2022.

KIM, T. J. et al. **Enhanced antioxidant capacity and antimicrobial activity of tannic acid by thermal processing.** Food Chemistry, v. 118, n. 3, p. 740–746, 2010.

KINOSHITA, K.; NAKAMURA, H. **eF-site and PDBjViewer: Database and viewer for protein functional sites.** Bioinformatics, v. 20, n. 8, p. 1329–1330, 2004.

LAKOWICZ, J. R. **Principles of fluorescence spectroscopy**. Third ed. Baltimore, Maryland, USA: Springer, 2006a.

LAKOWICZ, J. R. **Principles of Fluorescence Spectroscopy**. Trird edit ed. Maryland, USA: [s.n.].

LELIS, C. A. et al. **Binding thermodynamics of synthetic dye Allura Red with bovine serum albumin**. Food Chemistry, v. 217, p. 52–58, fev. 2017a.

LELIS, C. A. et al. **Determination of driving forces for bovine serum albumin-Ponceau4R binding using surface plasmon resonance and fluorescence spectroscopy: A comparative study**. Food Hydrocolloids, v. 70, p. 29–35, set. 2017b.

LEŚNIEROWSKI, G.; YANG, T. **Lysozyme and its modified forms: A critical appraisal of selected properties and potential. T**rends in Food Science and Technology, v. 107, n. August 2020, p. 333–342, 2021.

LESSCHAEVE, I.; NOBLE, A. C. P**olyphenols: factors influencing their sensory properties and their effects on food and beverage preferences.** The American journal of clinical nutrition, v. 81, n. 1 Suppl, p. 330–335, 2005.

LI, M. et al. **Bovine beta-casein micelles as delivery systems for hydrophobic flavonoids.** Food Hydrocolloids, v. 96, n. 17, p. 653–662, 2019.

LIU, X. et al. **Investigation of the interaction for three Citrus flavonoids and α-amylase by surface plasmon resonance.** Food Research International, v. 97, p. 1–6, jul. 2017.

LOU, W. et al. **Antioxidant and α-amylase inhibitory activities of tannic acid.** Journal of Food Science and Technology, v. 55, n. 9, p. 3640–3646, 2018.

LUO, J. et al. **Binding properties of marine bromophenols with human protein tyrosine phosphatase 1B: Molecular docking, surface plasmon resonance and cellular insulin resistance study.** International Journal of Biological Macromolecules, v. 163, p. 200–208, nov. 2020.

MAGALHÃES, O. F. et al. **Energetic and molecular dynamic characterization of lysozyme/β-carotene interaction. J**ournal of Molecular Liquids, v. 337, 2021a.

MIELCZAREK, C. **Acid–base properties of selected flavonoid glycosides.** European Journal of Pharmaceutical Sciences, v. 25, n. 2–3, p. 273–279, jun. 2005.

MOHAMMADI, F.; MOEENI, M. **Analysis of binding interaction of genistein and kaempferol with bovine α-lactalbumin.** Journal of Functional Foods, v. 12, p. 458–467, 2015a.

MOHAMMADI, F.; MOEENI, M. **Study on the interactions of trans-resveratrol and curcumin with bovine α-lactalbumin by spectroscopic analysis and molecular docking.** Materials Science and Engineering C, v. 50, p. 358–366, 2015b.

NAN, Z. et al. **Interaction of graphene oxide with bovine serum albumin: A fluorescence quenching study.** Spectrochimica Acta Part A: Molecular and Biomolecular Spectroscopy, v. 210, p. 348–354, mar. 2019.

NGUYEN, V. B. et al. **Porcine pancreatic α-amylase inhibitors from Euonymus laxiflorus Champ**. Research on Chemical Intermediates, v. 43, n. 1, p. 259–269, 2017.

NUNES, N. M. et al. **Interaction of cinnamic acid and methyl cinnamate with bovine serum albumin: A thermodynamic approach**. Food Chemistry, v. 237, p. 525–531, 2017.

NUNES, N. M. et al. **Surface plasmon resonance study of interaction between lactoferrin and naringin.** Food Chemistry**,** v. 297, n. April, p. 125022, 2019.

NUNES, N. M. et al. **Naringenin-lactoferrin binding: Impact on naringenin bitterness and thermodynamic characterization of the complex**. Food Chemistry, v. 331, n. June, p. 127337, 2020.

ONG, J. N.; HACKETT, D. A.; CHOW, C. **Sleep quality and duration following evening intake of alpha-lactalbumin : a pilot study**. Biological Rhythm Research, v. 1016, n. April, p. 0, 2017.

PACHECO, A. F. C. et al. **β-Casein monomers as potential flavonoids nanocarriers: Thermodynamics and kinetics of β-casein-naringin binding by fluorescence spectroscopy and surface plasmon resonance**. **I**nternational Dairy Journal, v. 108, 2020.

PAIVA, P. H. C. et al. **Influence of protein conformation and selected Hofmeister salts on bovine serum albumin/lutein complex formation.** Food Chemistry, v. 305, n. May 2019, p. 125463, 2020.

PERMYAKOV, E. A.; BERLINER, L. J. **α-Lactalbumin: structure and function.** FEBS Letters, v. 473, n. 3, p. 269–274, 2000.

PERUSKO, M. et al. **Antioxidative capacity and binding affinity of the complex of green tea catechin and beta-lactoglobulin glycated by the Maillard reaction**. Food Chemistry, v. 232, p. 744–752, 2017.

RASCHKA, S. et al. **Protein–ligand interfaces are polarized: discovery of a strong trend for intermolecular hydrogen bonds to favor donors on the protein side with implications for predicting and designing ligand complexes**. Journal of Computer-

Aided Molecular Design, v. 32, n. 4, p. 511–528, abr. 2018.

REZENDE, J. DE P. et al. **Polydiacetylene/triblock copolymer nanosensor for the detection of native and free bovine serum albumin**. Materials Science and Engineering: C, v. 70, p. 535–543, jan. 2017.

REZENDE, J. DE P. et al. T**hermodynamic and kinetic study of epigallocatechin-3-gallate-bovine lactoferrin complex formation determined by surface plasmon resonance (SPR): A comparative study with fluorescence spectroscopy**. **F**ood Hydrocolloids, v. 95, n. January, p. 526–532, 2019.

REZENDE, J. DE P. et al. **Human serum albumin-resveratrol complex formation: Effect of the phenolic chemical structure on the kinetic and thermodynamic parameters of the interactions.** Food Chemistry, v. 307, n. September 2019, p. 125514, 2020a.

REZENDE, J. DE P. et al. **Human serum albumin-resveratrol complex formation: Effect of the phenolic chemical structure on the kinetic and thermodynamic parameters of the interactions.** Food Chemistry, v. 307, n. May 2019, p. 125514, 2020b.

REZENDE, J. DE P. et al. **Temperature modulation of lutein-lysozyme hydrophobic-hydrophilic interaction balance.** Journal of Molecular Liquids, p. 113887, jul. 2020c.

ROMANO, A. et al. **Bovine alpha-lactalbumin assemblies with capsaicin : Formation , interactions , loading and physiochemical characterization.** Food Chemistry, v. 352, n. February, p. 129306, 2021.

SALEHI, B. et al. T**he Therapeutic Potential of Naringenin : A Review of Clinical Trials**. v. 26, n. Figure 1, p. 1–18, 2019.

SANTA ROSA, L. N. et al. **B-Lactoglobulin Conformation Influences Its Interaction With Caffeine.** Food Bioscience, v. 44, n. July, 2021.

SERES, D. S.; COATES, P. M. C**omment on "Western Dietary Pattern Antioxidant Intakes and Oxidative Stress: Importance during the SARS-CoV-2/COVID-19 Pandemic".** Advances in Nutrition, v. 12, n. 3, p. 1045–1046, 2021.

SHAIKH, S.; O'DONNELL, C. **Applications of fluorescence spectroscopy in dairy processing: a review.** Current Opinion in Food Science, v. 17, p. 16–24, out. 2017.

SOARES, S. et al. **Tannins in food: Insights into the molecular perception of astringency and bitter taste.** Molecules, v. 25, n. 11, p. 1–26, 2020.

SOUZA, F. R. et al. **Interaction of naringin and naringenin with DPPC monolayer at the air-water interface.** Colloids and Surfaces A: Physicochemical and Engineering Aspects, v. 584, p. 124024, jan. 2020.

STERLING, T.; IRWIN, J. J. ZINC 15 - **Ligand Discovery for Everyone.** Journal of Chemical Information and Modeling, v. 55, n. 11, p. 2324–2337, 2015.

SU, J. et al. **Effect of tannic acid on lysozyme activity through intermolecular noncovalent binding**. Journal of Agriculture and Food Research, v. 1, n. October, p. 100004, 2019.

SUN, L. et al. **Interactions between polyphenols in thinned young apples and porcine pancreatic α-amylase: Inhibition, detailed kinetics and fluorescence quenching.** Food Chemistry, v. 208, p. 51–60, 2016.

TAGASHIRA, A. et al. **Anti-inflammatory effect of lysozyme from hen egg white on mouse peritoneal macrophages**. Cytotechnology, v. 70, n. 3, p. 929–938, 2018.

VILCACUNDO, R. et al. **Antibacterial activity of hen egg white lysozyme denatured by thermal and chemical treatments**. Scientia Pharmaceutica, v. 86, n. 4, p. 1–17, 2018.

VIOLET, M.; MEUNIER, J. **Kinetic study of the irreversible thermal denaturation**

of Bacillus licheniformis a-amylase. v. 263, p. 665–670, 1989.

WANG, W.; ROBERTS, C. J. **Non-arrhenius protein aggregation.** AAPS Journal, v. 15, n. 3, p. 840–851, 2013.

WU, T. et al. **In vitro studies of Gynura divaricata (L.) DC extracts as inhibitors of key enzymes relevant for type 2 diabetes and hypertension.** Journal of Ethnopharmacology, v. 136, n. 2, p. 305–308, 2011.

WU, T. et al. **What is new in lysozyme research and its application in food industry? A review.** Food Chemistry, v. 274, n. September 2018, p. 698–709, 2019.

YANG, B. et al. **Characterization of bioactive recombinant human lysozyme expressed in milk of cloned transgenic cattle.** PLoS ONE, v. 6, n. 3, p. 1–10, 2011.

YEKTA, R. et al. **A new optical method to analyze ligand-protein interaction: affinity-based screening system.** Microchemical Journal, v. 157, p. 104910, set. 2020.

Supporting Information

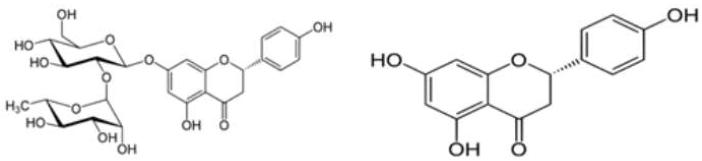

Fig. S1. Molecular structures of naringin (PubChem CID: 442428) and naringenin (PubChem CID: 439246).

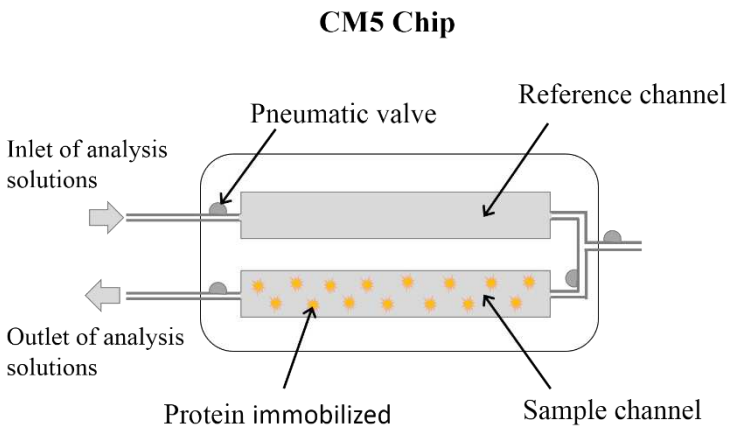

Fig. S2. Dual-channel microfluidic sensor chip: sample channel with immobilized protein and reference channel without ligand (schematically drawn).

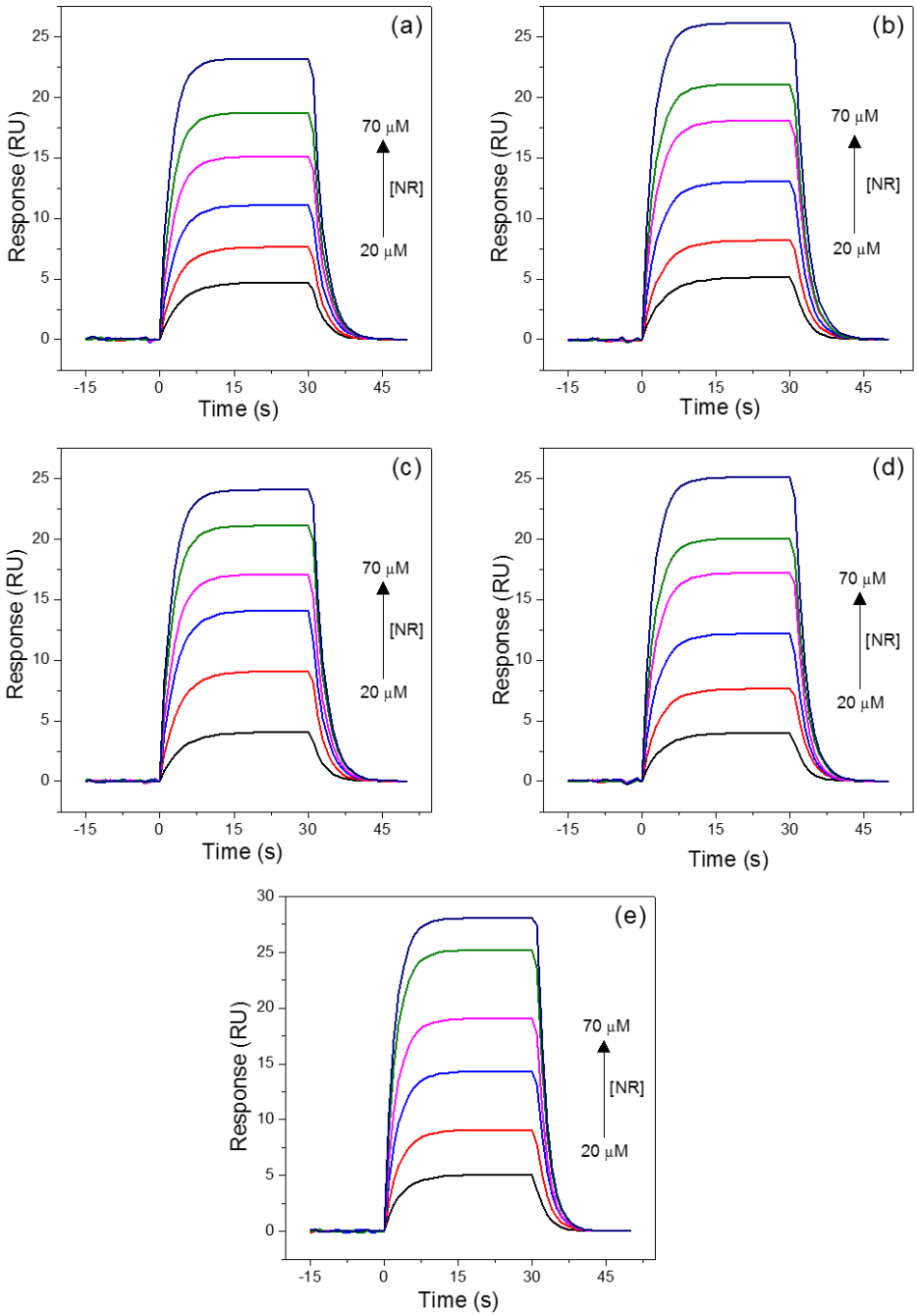

Fig. S3. SPR sensorgrams for $\alpha la - naringin$ binding to the low-density (4009 RU) α-lactalbumin CM5 chip surface, at (a) 285.15 K, (b) 289.15 K, (c) 293.15 K, (d) 297.15 K, and (e) 301.15 K. The arrow indicates increasing $naringin$ (NR) concentration from 20 to 70 μM (20, 30, 40, 50, 60 and 70 μM).

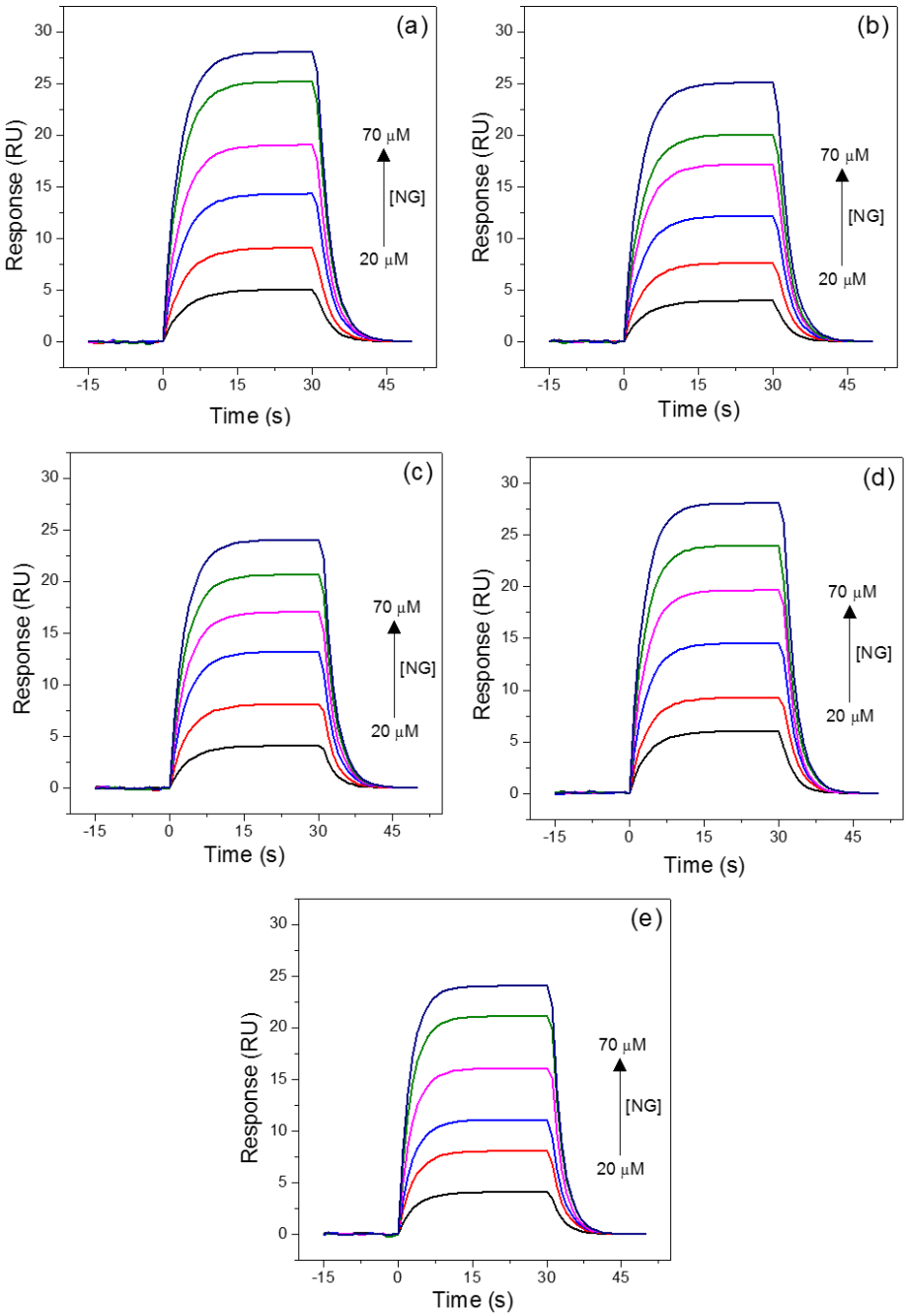

Fig. S4. SPR sensorgrams for $ala - naringenin$ binding to the low-density (4009 RU) α-lactalbumin CM5 chip surface, at (a) 285.15 K, (b) 289.15 K, (c) 293.15 K, (d) 297.15 K, and (e) 301.15 K. The arrow indicates increasing $naringenin$ (NG) concentration from 20 to 70 μM (20, 30, 40, 50, 60 and 70 μM).

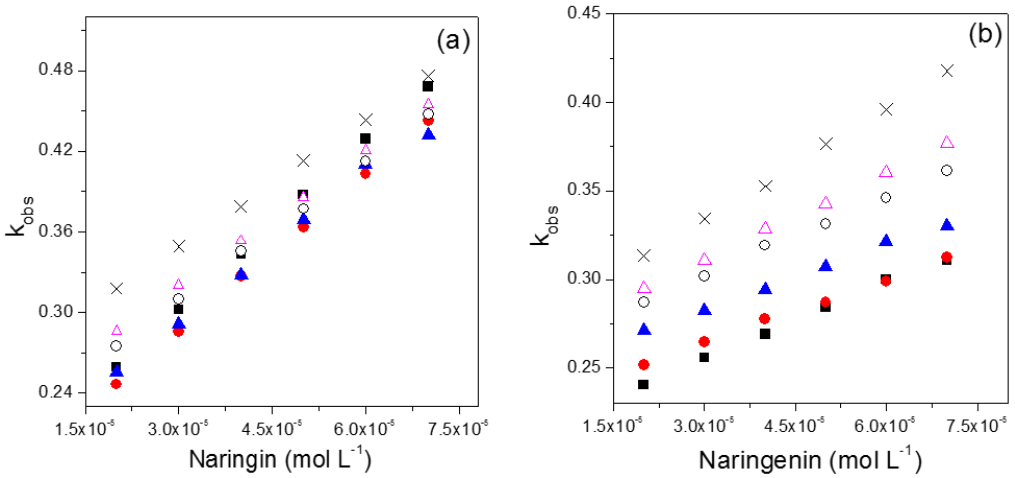

Fig. S5. The plot of k_{obs} as a function of polyphenol concentration used to determine k_{on} at temperatures: (■) 285.15 K, (●) 289.15 K, (▲) 293.15 K, (○) 297.15 K, (Δ) 298.15 K and (X) 301. 15 K: (a) $\alpha la - naringin$, and (b) $\alpha la - naringenin$.

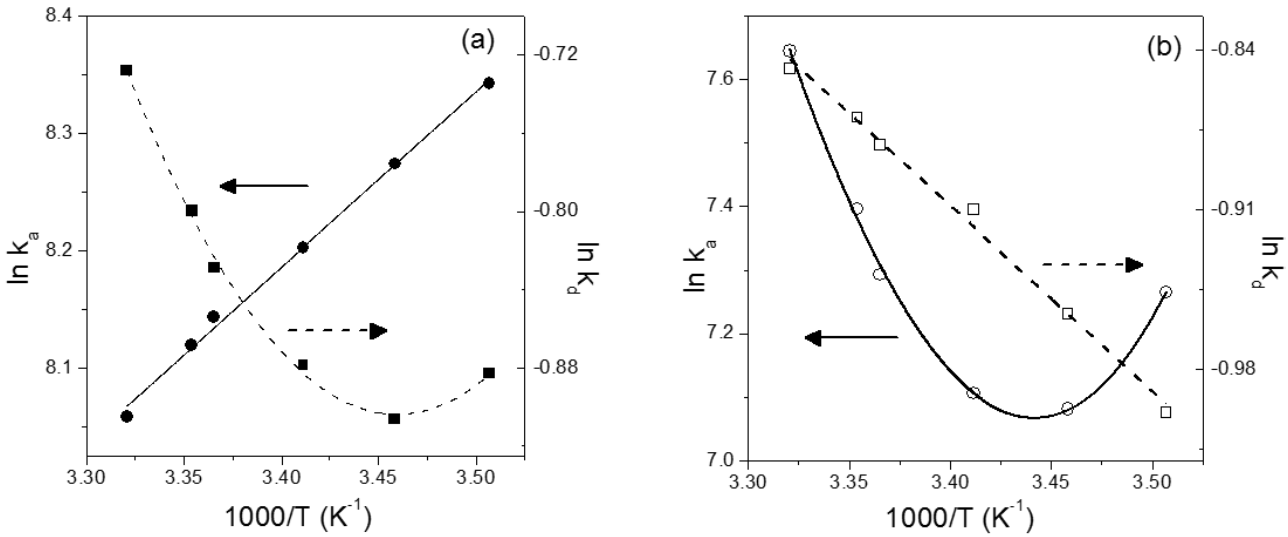

Fig. S6. Arrhenius plots for the association (k_{on}, ● and ○) and dissociation (k_{off}, ■ and □) of (a) $\alpha la - NR$ (closed symbol) and (b) $\alpha la - NG$ (open symbol).

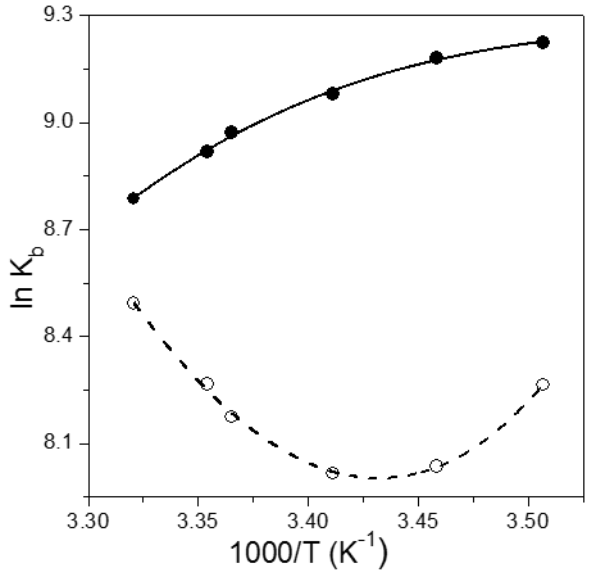

Fig. S7. The van't Hoff plots of ala interaction with $naringin$ (●) or $naringenin$ (○).

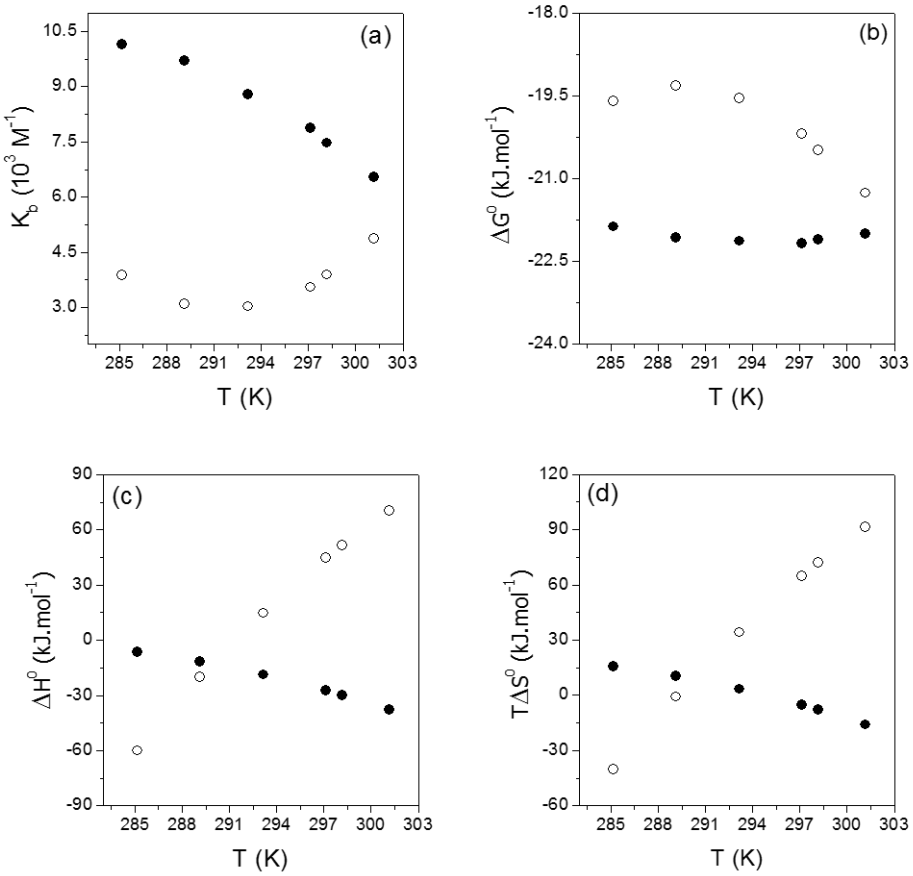

Fig. S8. Graphical relationship of thermodynamic parameters: (a) Binding constant (K_b); and standard changes in (b) Gibbs free energy (ΔG^0), (c) enthalpy (ΔH^0), and (d)

entropy ($T\Delta S^0$) for the formation of the $\alpha la - NR$ (●) and $\alpha la - NG$ (○) complexes in relation to temperature (T).

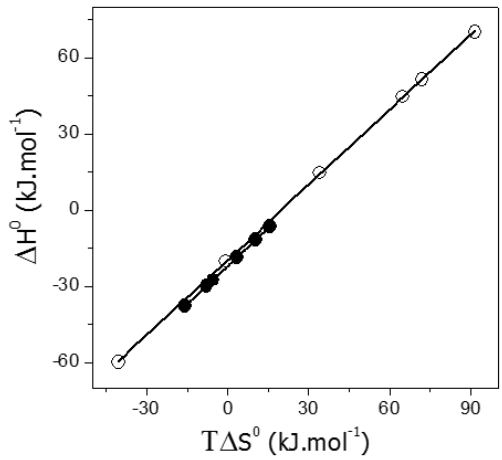

Fig. S9. Plot of enthalpy–entropy compensation, ΔH^0 versus $T\Delta S^0$, for the interactions of αla and $naringin$ (●) or $naringenin$ (○).

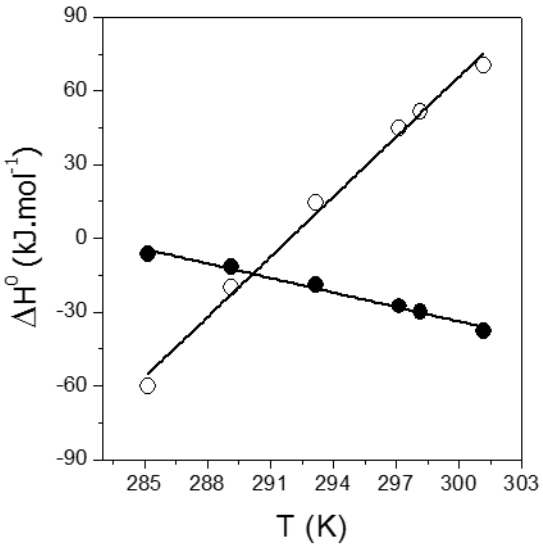

Fig. S10. Temperature dependence of ΔH^0 values for the formation of complexes between αla and $naringin$ (●) or $naringenin$ (○).

CONCLUSÃO GERAL

No capítulo 1, verificou-se por meio da técnica de espectroscopia de fluorescência que o ácido tânico (AT) é capaz de formar complexos estáveis com alfa-amilase (α-am), alfa-lactalbumina (α-La) e lisozima (Lys). O estudo termodinâmico revelou que a força motriz da interação AT-proteína, foram dependentes da estrutura química dos biopolímeros. O complexo α-am-AT foi formado por interações hidrofílicas, causadas principalmente pela formação de ligações de hidrogênio entre as moléculas de AT e os resíduos de aminoácidos de α-am. Para α-La-AT, as interações hidrofóbicas foram as principais responsáveis pela formação do complexo entre as duas moléculas. Finalmente, para o complexo Lys-AT, as interações hidrofílicas e hidrofóbicas contribuíram para a estabilização do complexo supramolecular. Esses resultados demonstram que a molécula de AT pode ser usada como uma “conexão” na construção de estruturas supramoleculares usando proteínas como unidades de construção.

No capítulo 2, analisando os resultados obtidos utilizando a técnica de Ressonância Plasmônica de superfície, foi possível concluir que houve interação entre a α-LA e Naringina (NR)/Naringenina (NG). As taxas de associação e dissociação entre α-La e NR foram maiores do que entre α-La e NG. Além disso, verificou-se que para NR, as interações hidrofílicas foram predominantes em todas as temperaturas avaliadas devido ao seu grupo glicosídeo constituinte. Também, o custo entrópico para acessar o sítio de ligação à proteína foi baixo, provavelmente mais próximo da interface da proteína em comparação com o sítio de interação para NG. Para a interação α-La e NG, à medida que a temperatura aumentou, o sítio α-La tornou-se cada vez mais flexível, favorecendo a penetração de NG em regiões mais hidrofóbicas de α-La. Isto é, o efeito hidrofóbico, potencializou ainda mais a interação entre as moléculas. Os modelos de ligação de NG e NR com α-La obtidos por *docking* molecular indicaram que o complexo α-La-NG foi mais estável que α-La-NR.

Em geral, os resultados contribuem para uma melhor compreensão da interação dos diferentes sistemas (AT-α-am, AT-α-La, AT-Lys, NR-α-La e NG-α-La) e da estabilidade dos complexos formados em diferentes temperaturas. Isto possibilita, otimizar e aperfeiçoar o uso desses complexos na indústria alimentícia, farmacêutica e de cosméticos.

REFERÊNCIAS

BAER-DUBOWSKA, W. et al. T**annic Acid: Specific Form of Tannins in Cancer Chemoprevention and Therapy-Old and New Applications.** Current Pharmacology Reports, v. 6, n. 2, p. 28–37, 2020.

BOUDET, A. M. **Evolution and current status of research in phenolic compounds.** Phytochemistry, v. 68, n. 22–24, p. 2722–2735, 2007.

BUITIMEA-CANTÚA, N. E.; GUTIÉRREZ-URIBE, J. A.; SERNA-SALDÍVAR, S. O. **Phenolic-protein interactions: Effects on food properties and health benefits.** Journal of Medicinal Food, v. 21, n. 2, p. 188–198, 2018.

DAS, S. et al. B**inding of naringin and naringenin with hen egg white lysozyme: A spectroscopic investigation and molecular docking study. Spectrochimica** Acta - Part A: Molecular and Biomolecular Spectroscopy, v. 192, p. 211–221, 2018.

ISHTIKHAR, M. et al. **Biophysical insight into the interaction mechanism of plant derived polyphenolic compound tannic acid with homologous mammalian serum albumins.** International Journal of Biological Macromolecules, v. 107, p. 2450–2464, 2018.

KACZMAREK, B. **Tannic acid with antiviral and antibacterial activity as a promising component of biomaterials-A minireview.** Materials, v. 13, n. 14, 2020.

KANDRA, L. et al. **Inhibitory effects of tannin on human salivary α-amylase**. Biochemical and Biophysical Research Communications, v. 319, n. 4, p. 1265–1271, 2004.

MAGALHÃES, O. F. et al. **Energetic and molecular dynamic characterization of lysozyme/β-carotene interaction**. Journal of Molecular Liquids, v. 337, p. 116404, set. 2021.

PERMYAKOV, E. A.; BERLINER, L. J. **α-Lactalbumin: structure and function.** FEBS Letters, v. 473, n. 3, p. 269–274, 2000.

REZENDE, J. DE P. et al. **Temperature modulation of lutein-lysozyme hydrophobic-hydrophilic interaction balance.** Journal of Molecular Liquids, p. 113887, jul. 2020.

SALEHI, B. et al. T**he Therapeutic Potential of Naringenin : A Review of Clinical Trials**. v. 26, n. Figure 1, p. 1–18, 2019.

SU, J. et al. **Effect of tannic acid on lysozyme activity through intermolecular noncovalent binding.** Journal of Agriculture and Food Research, v. 1, n. October, p. 100004, 2019.

YAZDANI, F. et al. **Structural insights into the binding behavior of flavonoids naringenin with Human Serum Albumin.** Journal of Molecular Liquids, v. 349, p. 118431, 2022.

BAER-DUBOWSKA, W. et al. **Tannic Acid: Specific Form of Tannins in Cancer Chemoprevention and Therapy-Old and New Applications**. Current Pharmacology Reports, v. 6, n. 2, p. 28–37, 2020.

BOUDET, A. M. E**volution and current status of research in phenolic compounds**. Phytochemistry, v. 68, n. 22–24, p. 2722–2735, 2007.

BUITIMEA-CANTÚA, N. E.; GUTIÉRREZ-URIBE, J. A.; SERNA-SALDÍVAR, S. O. **Phenolic-protein interactions: Effects on food properties and health benefits.** Journal of Medicinal Food, v. 21, n. 2, p. 188–198, 2018.

DAS, S. et al. **Binding of naringin and naringenin with hen egg white lysozyme: A spectroscopic investigation and molecular docking study.** Spectrochimica Acta - Part A: Molecular and Biomolecular Spectroscopy, v. 192, p. 211–221, 2018.

ISHTIKHAR, M. et al. **Biophysical insight into the interaction mechanism of plant derived polyphenolic compound tannic acid with homologous mammalian**

serum albumins. International Journal of Biological Macromolecules, v. 107, p. 2450–2464, 2018.

KACZMAREK, B. **Tannic acid with antiviral and antibacterial activity as a promising component of biomaterials-A minireview**. Materials, v. 13, n. 14, 2020.

KANDRA, L. et al. **Inhibitory effects of tannin on human salivary α-amylase**. Biochemical and Biophysical Research Communications, v. 319, n. 4, p. 1265–1271, 2004.

MAGALHÃES, O. F. et al. **Energetic and molecular dynamic characterization of lysozyme/β-carotene interaction**. Journal of Molecular Liquids, v. 337, p. 116404, set. 2021.

PACHECO, A. F. C. et al. **β-Casein monomers as potential flavonoids nanocarriers: Thermodynamics and kinetics of β-casein-naringin binding by fluorescence spectroscopy and surface plasmon resonance**. International Dairy Journal, v. 108, 2020.

PERMYAKOV, E. A.; BERLINER, L. J. **α-Lactalbumin: structure and function. FEBS Letters**, v. 473, n. 3, p. 269–274, 2000.

REZENDE, J. DE P. et al. **Temperature modulation of lutein-lysozyme hydrophobic-hydrophilic interaction balance**. Journal of Molecular Liquids, p. 113887, jul. 2020.

SALEHI, B. et al. **The Therapeutic Potential of Naringenin : A Review of Clinical Trials**. v. 26, n. Figure 1, p. 1–18, 2019.

SU, J. et al. **Effect of tannic acid on lysozyme activity through intermolecular noncovalent binding**. Journal of Agriculture and Food Research, v. 1, n. October, p. 100004, 2019.

YAZDANI, F. et al. **Structural insights into the binding behavior of flavonoids naringenin with Human Serum Albumin.** Journal of Molecular Liquids, v. 349, p. 118431, 2022.